Biogeosciences Discuss., 12, 8615–8690, 2015
www.biogeosciences-discuss.net/12/8615/2015/
doi:10.5194/bgd-12-8615-2015
© Author(s) 2015. CC Attribution 3.0 License.

Biogeosciences Discussions
Open Access

This discussion paper is/has been under review for the journal Biogeosciences (BG).
Please refer to the corresponding final paper in BG if available.

Latitudinal and temporal distributions of diatom populations in the pelagic waters of the Subantarctic and Polar Frontal Zones of the Southern Ocean and their role in the biological pump

A. S. Rigual-Hernández[1], T. W. Trull[2,3], S. G. Bray[2], A. Cortina[4], and L. K. Armand[1]

[1]Department of Biological Sciences, Macquarie University, North Ryde, NSW 2109, Australia
[2]Antarctic Climate and Ecosystems Cooperative Research Centre, University of Tasmania, Hobart, Tasmania 7001, Australia
[3]CSIRO Oceans and Atmosphere Flagship, Hobart, Tasmania 7001, Australia
[4]Department of Environmental Chemistry, IDAEA-CSIC, 08034 Barcelona, Spain

Received: 18 May 2015 – Accepted: 24 May 2015 – Published: 11 June 2015

Correspondence to: A. S. Rigual-Hernández (andres.rigualhernandez@mq.edu.au)

Published by Copernicus Publications on behalf of the European Geosciences Union.

Abstract

The Subantarctic and Polar Frontal zones (SAZ and PFZ) represent a large portion of the total area of the Southern Ocean and serve as a strong sink for atmospheric CO_2. These regions are central to hypotheses linking particle fluxes and climate change, yet multi-year records of modern flux and the organisms that control it are, for obvious reasons, rare. In this study, we examine two sediment trap records of the flux of diatoms and bulk components collected by two bottom-tethered sediment traps deployed at mesopelagic depths (~ 1 km) in the SAZ (two-year record) and in the PFZ (six-year record) along the 140° E meridian. These traps provide a direct measure of transfer below winter mixed layer depths, i.e. at depths where effective sequestration from the atmosphere occurs, in contrast to study of processes in the surface ocean. Total mass fluxes were about two-fold higher in the PFZ ($24 \pm 13\,g\,m^{-2}\,yr^{-1}$) than in the SAZ ($14 \pm 2\,g\,m^{-2}\,yr^{-1}$). Bulk chemical composition of the particle fluxes mirrored the composition of the distinct plankton communities of the surface layer, being dominated by carbonate in the SAZ and by biogenic silica in the PFZ. POC export was similar for the annual average at both sites (1.0 ± 0.1 and $0.8 \pm 0.4\,g\,m^{-2}\,yr^{-1}$, for the PFZ and SAZ, respectively), indicating that the particles in the SAZ were relatively POC rich. Seasonality in the particle export was more pronounced in the PFZ. Peak fluxes occurred during summer in the PFZ and during spring in the SAZ. The strong summer pulses in the PFZ are responsible for a large fraction of the variability in carbon sequestration from the atmosphere in this region. The latitudinal variation of the total diatom flux was found to be in line with the biogenic silica export with an annual flux of $31 \pm 5.5 \times 10^8$ valves $m^{-2}\,yr^{-1}$ at the PFZ compared to $0.5 \pm 0.4 \times 10^8\,m^{-2}\,yr^{-1}$ of the SAZ. *Fragilariopsis kerguelensis* dominated the annual diatom export at both sites (43 at the SAZ and 59 % in the PFZ). POC fluxes displayed a strong positive correlation with the relative contribution of a group of weakly-silicified and bloom-forming species in the PFZ. Several lines of evidence suggest that the development of these species during the growth season facilitates the formation of aggregates and carbon export.

BGD
12, 8615–8690, 2015

Our results confirm previous work suggesting that *F. kerguelensis* is a major aspect of the decoupling of the carbon and silicon cycles in the high-nutrient low-chlorophyll waters of the Southern Ocean.

1 Introduction

The Southern Ocean is a critical component of the Earth's ocean-climate system and plays a pivotal role in the global biogeochemical cycles of nutrients and carbon. Due to its unique meridional overturning circulation, deep waters are upwelled south of the Polar Front supplying the surface waters with nutrients and allowing the ventilation of carbon dioxide accumulated during centuries of deep-sea respiration (Anderson et al., 2002; Pollard et al., 2006). Strong interactions with the atmosphere transform the upwelled deep waters into bottom, intermediate, and mode waters, which spread to lower latitudes renewing the intermediate and abyssal depths of the world ocean (Sarmiento et al., 2004, 2010). Dissolution of carbon dioxide in these newly formed waters (i.e. the solubility pump) and the transport of photosynthetically fixed carbon to depth in settling particles (i.e. the biological pump) modulate the extent to which the carbon dioxide is transferred to the atmosphere. The balance between these processes determines the role of the Southern Ocean either as a source or sink of atmospheric CO_2 over glacial-interglacial climate cycles (Kohfeld et al., 2005; Anderson et al., 2009; Barker et al., 2009; Sigman et al., 2010).

At present, the Southern Ocean biological pump is not operating at its full capacity (De La Rocha, 2010). High concentrations of macronutrients coupled with only modest rates of primary production characterize its surface waters (Arrigo et al., 1998; Falkowski et al., 1998; Moore and Abbott, 2000; Arrigo et al., 2008). Low sun angles, deep wind-mixed surface waters and lack of the micronutrient iron restrict phytoplankton growth (Johnson et al., 1997; Fitzwater et al., 2000; Boyd et al., 2007; Venables and Moore, 2010) making the Southern Ocean the largest high nutrient low-chlorophyll (HNLC) region in the world ocean (Martin, 1990; Minas and Minas, 1992). However,

BGD
12, 8615–8690, 2015

there are exceptions to this situation with areas of higher phytoplankton abundance occurring along oceanographic fronts (Laubscher et al., 1993; Hense et al., 2000; Moore and Abbott, 2000), downstream of some islands (Blain et al., 2001; Park et al., 2010), in the wake of the retreating seasonal sea ice (Smith et al., 1988; Brzezinski et al., 2001), in coastal polynyas (Arrigo and van Dijken, 2003) and in coastal systems of Antarctica (de Baar et al., 1995; Sedwick et al., 2000; Brzezinski et al., 2001). In these areas iron fertilizes the surface layer triggering phytoplankton blooms in spring and summer.

Diatoms are a group of eukaryotic unicellular algae characterized by opaline silica tests (frustules) that can be preserved in the sedimentary record. They are one of the most abundant primary producers in the Southern Ocean and make the major contribution to the biogenic silica (BSi) content of deep-sea sediments. Satellite and in situ observations reveal that extensive diatom blooms occasionally develop in the Antarctic Circumpolar current (ACC; e.g. Kopczynska et al., 2001; Green and Sambrotto, 2006; Alvain et al., 2008; de Salas et al., 2011; Grigorov et al., 2014) which results in the formation of a band of siliceous ooze that encircles Antarctica (DeMaster, 1981; Buesseler et al., 2001; DeMaster, 2002). This "Diatom Ooze Belt" defined by Burckle and Cirilli (1987) constitutes the world's largest sedimentary sink for biogenic silica and accounts for about one third of the global biogenic silica accumulation (Tréguer and De La Rocha, 2013; Tréguer, 2014). Therefore, the production and export of diatoms in the Southern Ocean are critical components of the global cycling of silica, and potentially the biological carbon pump. Indeed there is evidence from silicon isotopes and other paleo-proxies that silica export in the Southern Ocean has varied, in concert with other biogeochemical changes and atmospheric CO_2 variations, over a range of timescales (Brzezinski et al., 2002; Matsumoto et al., 2002; Sarmiento et al., 2004).

Despite improvements during the last two decades, our understanding of temporal and spatial variability of diatom production in the Southern Ocean is still severely limited by undersampling. Owing to its remoteness and harsh conditions, in situ observations of the structure and composition of Southern Ocean ecosystems have been traditionally performed from research vessels. These studies are limited to short obser-

BGD
12, 8615–8690, 2015

vational periods and therefore are insufficient to characterize the seasonal and inter-annual variability of diatom populations and their contribution to primary production and export. Most of our current knowledge about the temporal and spatial dynamics of phytoplankton in the Southern Ocean waters derives from satellite observations and biogeochemical models (e.g. Moore et al., 1999; Moore and Abbott, 2000; Arrigo et al., 2008; Gregg and Rousseaux, 2014). Recently, advances in the interpretation of optical signals have allowed to determine the specific contribution of major phytoplankton groups (e.g., coccolithophores, phaeocystis-like, diatoms, etc.) to phytoplankton abundance on a global and regional scale (e.g. Alvain et al., 2005; Alvain et al., 2008; Raitsos et al., 2008; Hirata et al., 2009; Rousseaux and Gregg, 2012; Alvain et al., 2013). However, as a more complete picture of the structure of the planktonic communities emerges, it becomes evident that in order to determine the role of phytoplankton in the biological pump and biogeochemical cycles, it is of critical importance to distinguish not just among major taxonomic groups but also within them. In particular, recent studies have shown how variations in the composition of diatom communities, which exhibit a wide range of competitive strategies, contribute to the regulation of the stoichiometric relationship between elements such as carbon and silicon in the global ocean (Boyd et al., 2010; Assmy et al., 2013; Boyd, 2013; Quéguiner, 2013).

Bottom-tethered sediment traps have contributed significantly to our understanding of the particle transfer in open ocean ecosystems (e.g. Lampitt and Antia, 1997; Honjo et al., 2008; Romero and Armand, 2010). Materials collected by sediment traps enable the characterization of the seasonal and inter-annual variability of biogeochemical and micro-organism fluxes. They can be used to determine the timing and magnitude of phytoplankton blooms (e.g. Ziveri et al., 2000b; Romero et al., 2009a; Grigorov et al., 2014), calibrate the ecological preferences of planktonic species (e.g. Romero et al., 1999; Rigual-Hernández et al., 2010; Howard et al., 2011) and assess the potential of specific taxa for palaeoceanographic reconstructions in a particular study region (e.g. Leventer, 1991; Leventer and Dunbar, 1996; Gersonde and Zielinski, 2000; Romero et al., 2002; King and Howard, 2003, 2005; Romero et al., 2009b; Rigual-Hernández et

BGD
12, 8615–8690, 2015

al., 2012). Additionally, they provide details of the vectors responsible for sedimentation and their influence on the oceanic chemical budgets (e.g. Boyd and Newton, 1999; Ziveri et al., 2000a; Lampitt et al., 2009). For example, sediment trap studies in the Southern Ocean have revealed that the particle export in this region is highly seasonal and that maximum fluxes of particulate matter occur in areas under the influence of seasonal sea ice where diatoms are most abundant (e.g. Honjo et al., 2000; Suzuki et al., 2001; Fischer et al., 2002; Pilskaln et al., 2004; Grigorov et al., 2014). Other studies have revealed the crucial role of particular diatom species in driving the biological pump in naturally iron-fertilized waters, such as *Chaetoceros* resting spores around the Kerguelen Plateau (Rembauville et al., 2015) or the resting stages of *Eucampia antarctica* var. *antarctica* in the Crozet Island system (Salter et al., 2012). Most of these sediment trap experiments have been carried out in areas of relatively high primary production such as coastal systems and areas under the influence of seasonal sea ice. However very few experiments have been conducted in the pelagic province which, despite its relatively low phytoplankton abundance, is responsible for approximately 90 % of the annual primary production in the Southern Ocean due to its large size (Arrigo et al., 2008).

In this work we document the seasonal and inter-annual variability of the chemical (total mass, biogenic silica, carbonate and particulate organic carbon) and biological (diatom assemblages) composition of the material captured at two mooring sites along the 140° E, representative of a large proportion of the Subantarctic and Polar Frontal Zones of the Southern Ocean. The main objectives of this study are:

1. to document the latitudinal variations in the composition of the particle fluxes and diatom communities across sites.

2. to describe the pattern of total mass and major component fluxes in terms of seasonality and inter-annual variability in the Subantarctic zone (SAZ) and Polar Frontal zone (PFZ).

BGD
12, 8615–8690, 2015

3. to assess the role of the seasonal variability of diatom communities on the biological pump and cycling of silica.

4. to provide annual estimates of biogenic silica, carbonate, particulate organic carbon and diatom valve fluxes to the deep ocean for two major pelagic hydrological regions of the Southern Ocean.

2 Oceanographic and biological setting

The Southern Ocean is divided into concentric zones surrounding Antarctica by a series of frontal systems (Fig. 1), which are characterized by large geostrophic surface velocities (Orsi et al., 1995) and are linked to contours of sea surface height (SSH) (Sokolov and Rintoul, 2002, 2009b, a). Between these fronts lie zones of weak flow that tend to have relatively uniform water mass properties (Zentara and Kamykowski, 1981; Rintoul and Bullister, 1999) and biological distributions (Boyd, 2002; Thomalla et al., 2011). The Subantarctic Zone extends from the Subtropical front (STF) to the Subantarctic Front (SAF) and represents a transition zone between the subtropical gyres to the north and the Antarctic Circumpolar Current (AAC) to the south (Rintoul and Bullister, 1999). SAZ surface waters along $\sim 140^{\circ}$ E have summer SST's ranging between 8–12 °C whilst the mixed layer depth during winter can exceed 600 m (Rintoul and Trull, 2001). The SAF is characterised by a marked latitudinal surface gradient in temperature and salinity and, in the Australian sector, is split into two branches or filaments at mean latitudes of 50.5 and 52° S (Sokolov and Rintoul, 2002). The Polar Frontal Zone (PFZ) lies just south of the SAZ and represents the northernmost extent of the Antarctic waters. PFZ surface waters have summer SST's typically between 4–7 °C in summer, but the winter mixed layer is shallower (less than 200 m) than at the SAZ (Rintoul and Trull, 2001).

Together the SAZ and PFZ make up the Sub-Antarctic region (Fig. 1), which is the site of the formation of the Subantarctic Mode and Antarctic Intermediate Wa-

BGD
12, 8615–8690, 2015

ters (SAMW and AIW, respectively; McCartney, 1977). Both SAMW and AAIW are subducted northward beneath the subtropical gyres ventilating their lower thermocline (Sallée et al., 2006; Downes et al., 2009) and eventually supplying with nutrients the surface waters across the oceans of the southern hemisphere and North Atlantic (Sarmiento et al., 2004).

In terms of biogeochemical distributions, both zones can be defined as high nutrient-low chlorophyll (HNLC) regimes but with a remarkable difference between them. While PFZ surface waters are replete with phosphate, nitrate and silicate until at least mid-summer, in the SAZ silicate remains at low levels throughout the year (Rintoul and Trull, 2001; Wang et al., 2001). Dissolved iron concentrations in the mixed layer along the 140° E longitude transect are low and exhibit a decreasing trend with increasing latitude, with 0.27 ± 0.04 in the SAZ and 0.22 ± 0.02 nmol L^{-1} in the PFZ (Lannuzel et al., 2011). Primary production is thought to be co-limited by Fe supply and light in the PFZ and by Fe supply and low silicic acid concentration in the case of the SAZ (Boyd et al., 1999; Boyd et al., 2001; Lannuzel et al., 2011).

As a consequence of these different physical and biochemical properties, the SAZ and PFZ exhibit two distinct phytoplankton communities. SAZ surface waters are dominated by coccolithophores, other flagellates and cyanobacteria with lower abundances of diatoms. PFZ waters are also rich in coccolithophores and flagellates, but contain few cyanobacteria whereas diatoms are more abundant and of larger size (Deacon, 1982; Wright et al., 1996; Popp et al., 1999; Kopczynska et al., 2001; de Salas et al., 2011). Finally, it is worthy to note a feature present in the PFZ but not in the SAZ: a subsurface chlorophyll maximum (SCM) dominated by large diatom species (Kopczynska et al., 2001) has been consistently reported during summer in the PFZ within or beneath the seasonal pycnocline, probably formed as a response to iron and silicate colimitation (Popp et al., 1999; Parslow et al., 2001).

BGD
12, 8615–8690, 2015

3 Material and methods

3.1 Field experiment

A series of deep-moored sediment trap deployments was instigated in 1997 by the Australian SAZ program (Trull et al., 2001b) and now continues as a component of the Australian Integrated Marine Observing System Southern Ocean Time Series (Trull et al., 2010; Shadwick et al., 2015). Two sites representative of a large proportion of the SAZ and PFZ were occupied quasi-continuously for the decade 1997–2007. Both sites were located along the 140° E longitude: station 47° S was set on the abyssal plain of the central SAZ whereas station 54° S was placed on a bathymetric high of the Southeast Indian Ridge in the PFZ (Fig. 1; Table 1). Additionally, two other sites were instrumented over a one-year period, beneath the SAF (site 51° S, 1997–1998) and within the southern Antarctic Zone (site 61° S, 2001–2002). Here, we present data from the 47° S 1000 m trap between 1999–2001 (two-year record) and from the 54° S 800 m trap between 1997–2007 (six-year record). Biogenic particle flux data of sites 47, 51 and 54° S for the first year deployment (1997–1998) and of site 61° S for the year 2001–2002 have already been published in Trull et al. (2001a) and Rigual-Hernández et al. (2015), respectively.

All traps were MacLane Parflux sediment traps: conical in shape with a 0.5 m^2 opening area and equipped with a carrousel of 13 or 21 sampling cups. Cup rotation intervals were established based on anticipated mass fluxes. Shortest intervals corresponded with the austral summer and autumn ranging typically between 4.25 and 10 days, whereas the longest intervals were 60 days, corresponding with winter (Table 2). Each trap was paired with an Aanderaa current meter and temperature sensor. The 250 mL collection cups were filled with a buffered solution of sodium tetraborate (1 g L^{-1}), sodium chloride (5 g L^{-1}) and mercury chloride (3 g L^{-1}) in unfiltered deep seawater from the region (collected at 1200 m depth, 49°17° S, 153°58° E). Full details of the mooring designs can be found in Bray et al. (2000) and Trull et al. (2001a).

BGD
12, 8615–8690, 2015

3.2 Quality check of downward particle fluxes

Current speeds largely influence the efficiency with which sediment traps collect the particles sinking in the water column (Baker et al., 1988; Gust et al., 1992; Yu et al., 2001). The threshold of current velocity above which sinking particles are no longer quantitatively sampled is generally considered to be around 12 cm s^{-1} (Baker et al., 1988). Average current speeds for the whole sampling interval at the trap levels were lower than 11 cm s^{-1} for both sites, and therefore they seem to be non-critical for collection efficiencies. Additionally, radioisotope analyses of material from the first year deployment by Trull et al. (2001) provide some extra insights to assess the collection efficiency of the traps. The ^{230}Th flux/production ratios for the 1997–1998 deployment were 0.6 ± 0.1 and 0.7 ± 0.1 for the 47 and 54° S traps, respectively. These values suggest that some degree of undertrapping is likely to have occurred at both sites. However, as these values are almost identical for both traps, it can be assumed that the trapping efficiency did not account for the observed latitudinal variations in the magnitude of the particle export between sites. Taking into consideration all the above and the fact that the assessment of trapping efficiency from ^{230}Th alone is fraught with uncertainties (Trull et al., 2001a; Buesseler et al., 2007), trap fluxes were not corrected for possible undertrapping in the present study.

3.3 Determination of major constituents of the flux

A detailed description of the methodology used for the determination of the flux intensity and composition of settling particles for the first mooring deployments in 1997–1998 can be found in Bray et al. (2000) and Trull et al. (2001a). After recovery, sediment trap cups were allowed to settle before supernatant was drawn off with a syringe for salinity, nutrients and pH measurements. The remaining sample slurries were sieved through a 1 mm sieve and then split into 10 fractions using a rotary splitter (McLane, Inc.). Three of these splits were filtered onto Nucleopore filteres (0.45 pore size), removed from the filter as a wet cake of material, oven-dried at 60 °C and ground in a mortar.

BGD
12, 8615–8690, 2015

This material was used to determine the dry mass flux and the major components of the flux (particulate inorganic carbon, particulate organic carbon and biogenic silica). Particulate inorganic carbon (PIC) was determined by closed system acidification with phosphoric acid and coulometry. Particulate total carbon (PC) was determined by unacidified combustion using a CHN analyzer. Particulate organic carbon (POC) was calculated from PC by substraction of PIC. Total silicon and aluminium contents were estimated by HF/HNO_3 microwave digestion and inductively coupled plasma emissions spectrometry following the methodology described by Bray et al. (2000). Biogenic silica was determined from total silica by substracting lithogenic silica estimated by assuming a lithogenic Al / Si mass ratio of 3.42 (Taylor, 1964). These methods for PIC and POC/PON were used for all subsequent years, with very slight modifications: (i) the wet cake method was replaced by drying prior to removing the material from the filter, (ii) in some years sieving and filtering was done at sea and the samples were frozen on the filters until dried on return to land. The silica methods varied more strongly over time: (i) for deployments beginning in 1998, 1999, and 2000, the use of HF in the digestion was replaced by high temperature combustion with lithium borate in a graphite crucible and HNO_3 digestion to determine total Si and Al, (ii) biogenic silica for these years (and retroactively for 1997) was calculated using the updated estimate for the lithogenic Al / Si mass ratio of 3.83 (Taylor and McLennan, 1985), (iii) from 2001 onwards, total silica was not measured, instead hot alkaline digestion and colorimetry was used to estimate biogenic silica directly (following the method of Quéguiner, 2001).

3.4 Siliceous microplankton sample preparation

A total of 138 samples were processed for siliceous microplankton analysis. Each split was refilled with distilled water to 40 mL, from which 10 mL were subsampled and buffered with a solution of sodium carbonate and sodium hydrogen carbonate (pH 8) and stored at 4 °C in the dark for future calcareous nannoplankton analysis. The remaining 30 mL were treated with potassium permanganate, hydrogen peroxide, and concentrated hydrochloric acid following the methodology used by (Romero et al.,

BGD
12, 8615–8690, 2015

1999). Three slides per sample were prepared and mounted using the standard decantation method outlined by Bárcena and Abrantes (1998). This method produces random settling of the diatom valves for quantitative microscopic purposes. Siliceous microplankton analysis was carried out on permanent slides (Norland optical adhesive 61 mounting medium; refractive index: 1.56) of acid-cleaned material. Qualitative and quantitative analysis were done at *x*1000 and *x*400 magnifications using an Olympus BH-2 compound light optical microscope with phase-contrast illumination. In order to properly characterize the diatom assemblages, a target of 400 diatom valves was counted per sample. Owing to the strong seasonality in diatom production, some cups collected very low numbers of diatom valves. For these samples a compromise between number to be counted and time spent had to be reached but the number of valves counted was never less than 100 with the exception of Cup 6 of year 2000–2001, and cup 14 of year 1999–2000 at the 47° S site which were not considered for relative abundance calculations due to their negligible diatom content. The resulting counts yielded estimates of specimens m^{-2} d^{-1} according to Sancetta and Calvert (1988) and Romero et al. (2009b), as well as relative abundances of diatom taxa.

3.5 Taxonomic identifications

All diatom and silicoflagellate specimens were identified to the lowest taxonomic level possible. Radiolarians were only identified at group level. Scanning Electron Microscope imagery was used on selected samples to verify taxonomic identifications made with the light microscope. Taxonomy followed modern concepts in Hasle and Syvertsen (1997). The resting spores of members of the subgenus *Hyalochaete* of the genus *Chaetoceros* were identified only at group level due to a lack of morphological criteria. The differentiation between *Pseudo-nitzschia lineola* and *Pseudo-nitzschia turgiduloides* was often difficult due to their state of preservation in the samples, therefore, they were grouped under the category *Pseudo-nitzschia* cf. *lineola* in this study. A species or group of species of the genus *Thalassiosira* larger than 20 µm, highly dissolved and with radial to fasciculated areolation were grouped together under the name *Tha-*

BGD
12, 8615–8690, 2015

lassiosira sp. 1. Several small *Thalassiosira* species with similar morphological features were assembled together under *Thalassiosira trifulta* group following Shiono and Koizumi (2000). Due to the gradational nature of the morphology between *Thalassiosira gracilis* var. *gracilis* and *T. gracilis* var. *expecta*, both varieties were grouped together under the name *T. gracilis* group following the recommendations of Crosta et al. (2005).

3.6 Statistical analysis

In order to enable comparison with other sites, annual flux estimates are provided in Table 3. These were obtained by assuming that total mass flux outside of the sampling period was constant and by linearly interpolating values for the small gaps (i.e. 8.5 to 17 days intervals) during the productive season. No attempt was made to annualize the relative contribution of the diatom taxa, and therefore average values of the integrated diatom assemblage for whole sampling interval are provided in Table 3.

In order to investigate the covariability between the main diatom taxa along our sediment trap records, we conducted separate principal component analyses (PCA) for each site using of Statistica 7.0® software. PCA analysis is a statistical technique that reduces the information brought by a high number of independent variables into smaller set of dimensions (factors) with a minimum loss of information. Only species and taxonomic groups with relative contributions >1 % for the entire sampling period were considered in the analysis, i.e. thirteen taxa from site 47° S and nine taxa from site 54° S. The relative contribution of these groups of species was recalculated for each sample and then a log-transformation (log x+1) was applied in order to normalize the distribution of the data. Diatom groups were then determined using a Q-mode factor analysis of the samples with a maximized variance (VARIMAX) rotation.

The Shannon's diversity index (Shannon, 1949) was used to document latitudinal diversity trends across sites (Table 4).

BGD
12, 8615–8690, 2015

3.7 Environmental variables

Weekly Sea-surface temperatures (SST) for the decade 1997–2007 were derived from the IGOSS NMC (the Integrated Global Ocean Services System Products Bulletin, National Meteorological Center; Reynolds et al., 2002) database, each value is a weekly composite of data collected within the area 48.5–45.5° S × 130–150° E for the 47° S site and 55.5–52.5° S × 130–150° E for the 54° S site (Figs. 2a and 3a). Sea-WIFS satellite-derived chlorophyll *a* and photo-synthetically active radiation (PAR) estimates were obtained from NASA's Giovanni online data system (Acker and Leptoukh, 2007) for the same area used for the SST estimates (Figs. 2a and 3a).

Primary productivity values (mg C m^{-2} d^{-1}) for all the sites were obtained from the Ocean Productivity site (www.science.oregonstate.edu/ocean.productivity/index.php), which provides estimates of net primary productivity derived from SeaWIFS satellite data by the standard vertically generalized production model (VGPM; Behrenfeld and Falkowski, 1997) and the carbon-based production model (CbPM; Behrenfeld et al., 2005).

4 Results

A description of the total particle flux and its chemical signature at stations 47 and 54° S for the first year deployment of the sediment traps (1997–1998) can be found in Trull et al. (2001). Here, we present the chemical (total mass, biogenic silica, carbonate and POC) and biological (diatom species) compositions of the particle fluxes registered at ~ 1000 m at the 47° S site during two years (July 1999–October 2001) and at 54° S site during six years (September 1997–February 1998, July 1999–August 2000, November 2002–October 2004 and December 2005–October 2007; Table 2).

BGD
12, 8615–8690, 2015

4.1 Biogeochemical fluxes

The total mass and bulk component (biogenic silica, carbonate and POC) fluxes for both traps are shown in Figs. 2b and 3b and listed in Table 2. Annual total mass flux at ~1 km depth was lowest at station 47° S ($14 \pm 2\,g\,m^{-2}\,yr^{-1}$; two-year average ± standard deviation) and highest at station 54° S ($24 \pm 13\,g\,m^{-2}\,yr^{-1}$; six-year average ± standard deviation; Table 3). Biogenic silica (BSi) flux followed a similar latitudinal trend with lower fluxes at 47° S ($1 \pm 0\,g\,m^{-2}\,yr^{-1}$) compared to 54° S ($12 \pm 9\,g\,m^{-2}\,yr^{-1}$). Carbonate export exhibited less variability between sites, with values somewhat higher at 47° S ($10 \pm 3\,g\,m^{-2}\,yr^{-1}$) than those measured at 54° S ($7 \pm 3\,g\,m^{-2}\,yr^{-1}$, respectively). Interestingly, despite the strong latitudinal differences in the magnitude of the mass fluxes, POC export was very similar at both stations (1.0 ± 0.1 and $0.8 \pm 0.4\,g\,m^{-2}\,yr^{-1}$, for 47 and 54° S, respectively).

In terms of relative abundance, the biogenic silica fraction represented 57 % of the mass flux at the 54° S site whereas its contribution dramatically dropped to 7 % at the 47° S station. Calcium carbonate and POC accounted for 70 and 7.3 % at the 47° S site, respectively and 21 and 3 % at the 54° S station (Table 3). These differences were primarily driven by the northward decrease in the biogenic silica fluxes. The BSi : PIC mole ratios decreased northward mirroring the latitudinal variations of the particle composition, from 5.4 at station 54° S to 0.2 at station 47° S (Table 3). The POC : BSi followed an opposite pattern with 0.3 at 54° S and 4.9 at 47° S.

The seasonality of the total mass flux at station 47° S during the two-year record showed a period of enhanced particle export in spring and secondary peaks in summer and autumn (Fig. 2b). The highest fluxes were registered in November–December 2000 ($92–176\,mg\,m^{-2}\,d^{-1}$), March 2001 ($105\,mg\,m^{-2}\,d^{-1}$) and October 1999 ($90\,mg\,m^{-2}\,d^{-1}$). Total mass flux at the 54° S site was strongly seasonal with maximum values occurring during the late spring-summer and very low export prevailing through the autumn and winter months. The late spring-summer export maxima were as short as three months and often showed a bimodal distribution (e.g.

BGD
12, 8615–8690, 2015

1997–1998, 1999–2000, 2002–2003; Fig. 3b). The highest total mass fluxes at this site were collected during December-January 1999 (511–724 mg m^{-2} d^{-1}), January 2006 (418 mg m^{-2} d^{-1}), February 2003 (397 mg m^{-2} d^{-1}) and January 1998 (396 mg m^{-2} d^{-1}).

4.2 Diatom fluxes

The biogenic silica flux at the 47 and 54° S site was composed of diatoms, silicoflagellates, radiolarians, and a handful of skeletons of the dinoflagellate *Actiniscus pentasterias*. Diatom fluxes were one order of magnitude higher than those of silicoflagellates and radiolarians at the 47° S site, and one and three orders of magnitude higher, respectively, at the 54° S site. Consistent with the biogenic silica flux, diatoms were most numerous in the 54° S site with an annual flux of 31 ± 5.5 10^8 valves m^{-2} yr^{-1} (six-year average ± standard deviation) compared to 0.5 ± 0.4 10^8 valves m^{-2} yr^{-1} (two-year average ± standard deviation) of the 47° S site.

Total diatom valve flux at the 47° S site (Fig. 4a) showed a less pronounced seasonality than that observed at 54° S (Fig. 5a) and exhibited a weak correlation with the total mass ($r = 0.37$, $n = 30$) and BSi ($r = 0.42$, $n = 29$) fluxes. Diatoms occurred in greatest numbers during November 2000 (1.6×10^6 valves m^{-2} d^{-1}), February–March 2001 ($0.4–0.8 \times 10^6$ valves m^{-2} d^{-1}) and October 1999 (0.4×10^6 valves m^{-2} d^{-1}).

At station 54° S, total diatom valve flux was highly seasonal and followed a similar pattern to that of the total mass ($r = 0.66$, $n = 108$) and BSi fluxes ($r = 0.68$, $n = 108$). These correlations are high despite the biases associated to our diatom valve counting technique which does not allow quantification of small valve fragments. In particular the high diatom-valve fragmentation observed during the productive period of 1999–2000 reduced the correlations between diatom valve flux and total mass and biogenic silica fluxes. In fact, the latter correlations increased significantly after excluding the 1999–2000 data ($r = 0.85$, $n = 88$ and $r = 0.87$, $n = 88$, respectively).

The spring-summer diatom bloom often exhibited two peaks of enhanced export separated by a period of lower flux (e.g. 1997–1998, 1999–2000, 2002–2003; Figs. 5a

BGD
12, 8615–8690, 2015

and 7). During the productive period of 2006–2007, the diatom bloom exhibited one single peak during which the largest diatom fluxes of the record were registered (up to 100×10^6 valves m^{-2} d^{-1} in January 2007; Fig. 5a). Secondary diatom flux maxima were registered in January 1998 (71×10^6 valves m^{-2} d^{-1}), December 2002 (65×10^6 valves m^{-2} d^{-1}) and December 1999 (52×10^6 valves m^{-2} d^{-1}). We noticed that during the 1999–2000 summer bloom the high BSi fluxes were not coupled with a proportional increase of the diatom valves (Fig. 5a). The higher degree of fragmentation observed on these samples could be attributed to either a more intense grazing pressure by the zooplankton community that year or by a higher fragmentation of the valves during the sample preparation due to the presence of abundant numbers of weakly silicified diatoms (e.g. species of the genus *Pseudo-nitzschia*) which are more prone to break during the sample processing (Rembauville et al., 2015).

In terms of diatom assemblage composition, the occurrence and fractional contributions of all the diatom taxa found at the 47 and 54° S study sites, as well as at 61° S (Rigual-Hernández et al., 2015) are provided in Table 4. The diatom sinking assemblage at station 47° S was more diversified ($H' = 2.48$) than those found south the SAF ($H' = 1.86$ at the 54° S; $H' = 1.04$ at the 61° S) consisting of 79 species or groups of species. The most abundant species was *Fragilariopsis kerguelensis*, which represented 43 % of the integrated assemblage (Fig. 4). Subordinate contributions to the diatom assemblage were made by *Azpeitia tabularis* (10 %), *Thalassiosira* sp. 1 (4 %), *Nitzschia bicapitata* (4 %), resting spores of *Chaetoceros* spp. (subgenus *Hyalochaetae*) (3 %), *Thalassiosira oestrupii* var. *oestrupii* (3 %), *Hemidiscus cuneiformis* (3 %) and *Roperia tesselata* (3 %; Fig. 4). A total of 77 taxa were identified at the 54° S site (Table 4). *F. kerguelensis* was also the dominant species, contributing up to 59 % of the diatom assemblage for the whole sampling period (Fig. 5). Secondary contributors correspond to *Pseudo-nitzschia* cf. *lineola* (8 %), *Pseudo-nitzschia heimii* (5 %), *Thalassiosira gracilis* group (4 %), *Fragilariopsis pseudonana* (3 %), *Fragilariopsis rhombica* (2 %) and *Thalassiosira lentiginosa* (2 %; Fig. 5).

BGD
12, 8615–8690, 2015

4.3 Principal component analysis

The PCA for the 47° S site identified 4 components containing 64 % of the total variance whereas that of the 54° S site required three components to describe 79 % of the information of diatom data (Table 5). Components 3 and 4 for 47° S and component 3 for 54° S explained only 13–14 % of the variance, were mostly monospecific and had no clear ecological significance. Therefore, we used only the first and second axes of the PCA that explain 38 and 65 % of the variance for the 47 and 54° S sites, respectively. Figure 6 shows the position of the species on the first two PCA axes for the 47 and 54° S sites. Together with the species, we plotted total and major components mass fluxes.

The first component of the PCA for the 47° S site (19 % of the variance) was dominated by the open ocean species *N. bicapitata* (Table 5). This species had a negative loading on factor 1 and showed its highest annual relative contribution during the autumn and winter months. The centric species *Azpeitia tabularis* and *Hemidiscus cuneiformis* (Fig. 6) had a positive loading on factor 1 and showed their highest relative abundance during spring and summer (Fig. 4). Factor 2 explained 19 % of the variance and was dominated by *F. kerguelensis*, *T. oestrupii* var. *oestrupii* and *Thalassiosira* sp. 1. *Fragilariopsis kerguelensis* maintained a relatively constant contribution to the diatom assemblages during the whole sampling interval with a tendency to peak in late-summer and autumn together with *T. oestrupii* var. *oestrupii*. *Thalassiosira* sp. 1 had a positive contribution to factor 2 and its maximum relative contribution occurred in late winter and spring. None of the factors of the PCA of the 47° S site were significantly correlated with the biogenic particle fluxes (Fig. 6a and Table 6a).

At the 54° S site, the first component (48 % of the total variance) was highly correlated with the bulk components of the flux (Fig. 6b and Table 6b) and individualizes two groups of diatom species which are defined by high absolute values of factor loadings. High-positive factor loadings characterize the bloom-forming *Pseudo-nitzschia* cf. *lineola*, *F. rhombica*, *F. pseudonana* and *N. directa* and the cool-open-ocean diatom

BGD
12, 8615–8690, 2015

T. gracilis group. The relative contribution of these species peaked during the productive season (Fig. 5) and showed a strong correlation with all the components of the flux (Fig. 6b and Table 6b). Therefore, diatom species characterized by a high-positive first factor loading can be defined as the "High-export group". In contrast, a high-negative factor loading on the first PCA axis was attributed to *F. kerguelensis*. The relative contribution of *F. kerguelensis* peaked during winter and autumn, coinciding with very low particle fluxes. *Pseudo-nitzschia heimii* was the only species with a high positive factor loading on the second PCA axis (Fig. 6b and Table 5) and its relative abundance peaked mainly from mid-summer to autumn. *Thalassiosira lentiginosa* had a high-negative factor loading in factor 2 and its maximum relative abundances occurred mainly during spring and autumn.

With the exception of year 2002–2003, a consistent diatom species succession was consistently observed over the growth season at the 54° S site (Figs. 5b and 7). During those years with a double-peak diatom sedimentation bloom, the first maximum (November to early-December) was always dominated by *F. kerguelensis* and by other large and heavily silicified diatoms, such as *T. lentiginosa*. During the second peak (in late-December to early-February), relative contribution of *Pseudo-nitzchia* cf. *lineola* and small *Fragilariopsis* species increased sharply, representing together up to 60 % of the diatom assemblage in January 2000 (Figs. 5b and 7). Even during year 2006–2007, when the diatom sedimentation bloom exhibited a single maximum, a similar succession can be discerned within the peak.

5 Discussion

5.1 Latitudinal trend of biogenic particle fluxes to the ocean interior

The contrasting latitudinal variations in the composition and magnitude of the particle fluxes along the 140° E transect reflect the physicochemical and biological distributions of the different zonal systems sampled by the traps. Relatively low BSi and diatom

BGD
12, 8615–8690, 2015

export measured in the mesopelagic waters of the SAZ (Fig. 8a and Table 3) are consistent with the low-to-moderate diatom biomass accumulation in the surface layer of this region (Kopczynska et al., 2001; de Salas et al., 2011). Low silicic acid (Smith Jr et al., 2000; Trull et al., 2001a; Wang et al., 2001; Bowie et al., 2011a) and iron levels (Sedwick et al., 1997; Sedwick et al., 2008; Bowie et al., 2009; Mongin et al., 2011), together with light limitation, as a result of cloudiness (Bishop and Rossow, 1991) and deep summer mixed layers (70–100 m, Rintoul and Trull, 2001), are considered the main factors responsible for the reduced diatom production in the SAZ. Moreover, the low BSi : PIC mole ratios measured by the traps ($<<1$; Table 3) illustrate the relatively low contribution of diatoms to the particle flux export to the ocean interior. Low diatom export fluxes and BSi : PIC mole ratios are characteristic of carbonate-dominated and low-productivity regimes (Honjo et al., 2008) and typical of much of the circumpolar SAZ (Honjo et al., 2000; Trull et al., 2001a).

The higher diatom valve fluxes and BSi export at the 54° S site (Table 3; Fig. 8a) agrees well with previous studies of the PFZ surface waters south of Tasmania, which reported relatively large and heavily silicified diatoms as major contributors to the phytoplankton biomass (Kopczynska et al., 2001; de Salas et al., 2011). Higher levels of silicic acid (Smith Jr et al., 2000), colder summer surface waters and shallower mixed winter layers than those of the SAZ (Rintoul and Trull, 2001) are most likely the main factors responsible for the greater prevalence of diatoms in this region. As a result of the enhanced diatom production and the drop in the abundance of calcifying phytoplankton (Nishida, 1986; Findlay and Giraudeau, 2000; Honjo et al., 2000), BSi : PIC mole ratios of the settling material at this site shift to >1 (Table 3).

Further south, at station 61° S in the southern AZ, Rigual-Hernández et al. (2015) documented an annual diatom flux one order of magnitude greater than that measured at the 54° S site (243×10^8 valves m^{-2} d^{-1} at 2000 m; Table 3 and Fig. 8a). The corresponding BSi export was as large as 65 g m^{-2} yr^{-1}, a value very similar to that reported in the AZ south New Zealand by Honjo et al. (2000; 57 g m^{-2}, station MS-4; Fig. 1). These very high BSi fluxes are arguably the largest BSi exports ever measured in the

BGD
12, 8615–8690, 2015

world's ocean (Honjo et al., 2008). Due to the upwelling of Circumpolar Deep Waters (CDW) at the Antarctic Divergence, the surface waters of the southern AZ exhibit very high silicate concentrations (up to 70 mmol Si m^{-3}; Pollard et al., 2006) which enhance diatom growth at the expense of other phytoplankton groups (Mengelt et al., 2001; Selph et al., 2001). These high diatom export values are consistent with the large accumulation of diatom remains in the surface sediments between the PF and the winter sea-ice edge that encircles Antarctica, the so-called Diatom Ooze Belt (Burckle and Cirilli, 1987). This Diatom Ooze Belt constitutes the single most important sink for silica in the world ocean (DeMaster, 1981; Ledford-Hoffman et al., 1986; Tréguer et al., 1995; Tréguer, 2014).

5.2 Latitudinal diatom species distribution

The species occurrence observed along the 140° E sediment trap transect is consistent with previous reports on diatom assemblage composition in the surface waters (Kozlova, 1966; Kopczynska et al., 1986; Kopczynska et al., 2001; de Salas et al., 2011) and sediments (Armand et al., 2005; Crosta et al., 2005; Romero et al., 2005) of the Australian sector of the Southern Ocean and provide evidence, once again, that the frontal systems represent natural physical boundaries for phytoplankton species distribution (Boyd, 2002).

Overall, the diatom assemblage registered at the 47° S site is typical of the SAZ and differs significantly from those found in the PFZ and AZ (Table 4). The SAZ represents a "buffer zone" between the subtropical gyres to the north and the polar waters to the south which results in a highly diverse diatom community as highlighted by the highest H' (2.48; Table 4) of the study transect. The occurrence of the warm water taxa *Hemidiscus cuneiformis*, *Fragilariopsis doliolus*, *Nitzschia kolaczeckii* and *Thalassiosira lineata* (Romero et al., 2002, 2005; Venrick et al., 2008) is restricted to this station, and therefore, these species appear as good indicators for the southward migration of the warmer, saltier and nutrient-poorer water masses of the SAZ into the ACC. Moreover, the stark increase in the abundance of the open-ocean diatoms *Azpeitia*

BGD
12, 8615–8690, 2015

tabularis, *Nitzschia bicapitata*, *Nitzschia braarudii*, *Rhizosolenia bergonii*, *Roperia tesselata*, *Thalassiosira eccentrica, Thalassiosira oestrupii* and *Thalassiosira symmetrica* north of the SAF suggest the preference of these species for warmer waters as already suggested by Hasle and Syvertsen (1997) and Romero et al. (2005). Since *Chaetoceros* resting spores are generally regarded as indicators of coastal environments (Abrantes, 1988; Treppke et al., 1996; Crosta et al., 1997; Takahashi et al., 2002; Rigual-Hernández et al., 2013), their presence at the 47° S site suggests that they could have been advected from a coastal region rather than having autochthonous origin. This concept is further supported by the significant correlation ($r = 0.7$, $n = 31$) between the fluxes of the coastal species group (*Cocconeis* spp. *Diploneis bombus* and *Paralia* spp.) and those of *Chaetoceros* RS. Some influence of coastal and subtropical waters over the study area is possible, as eddies from the East Australia Current and intermediate waters from the Tasman Outflow (a remnant of the East Australian Current) have been reported to extend as far south as the SAZ (Ridgway and Dunn, 2007; Herraiz-Borreguero and Rintoul, 2010; Herraiz-Borreguero and Rintoul, 2011). Thus, we interpret the occurrence of *Chaetoceros* RS and coastal taxa in the 47° S site as the advection of hemipelagic and/or neritic water masses from the Tasmanian shelf.

The sinking diatom assemblage registered at the 54° S site is characteristic of the cold and iron-limited waters of the ACC and largely defined by the dominance of *Fragilariopsis kerguelensis*. The relative abundance of *F. kerguelensis* at the PFZ (59 %) represents a transitional value between that of the AZ (80 %) and that of the SAZ (43 %). This strong latitudinal gradient mirrors its distribution in the surface sediments, which has been previously tied to summer SST (Crosta et al., 2005; Esper et al., 2010). However, other potentially important influences such as mixed layer depth, seasonality, and iron and silicate abundance also exhibit latitudinal gradients and therefore may also influence the distribution of this species. Peak abundances of *Pseudo-nitzschia* species (*P-n. heimii* and *Pseudo-nitzschia* cf. *lineola*) along the 140° E transect are observed in the PFZ (Table 4) and are consistent with previous studies that described this genus as a major contributor to the bulk phytoplankton biomass in the ACC waters

BGD
12, 8615–8690, 2015

(e.g. Kopczynska et al., 2001; Smetacek et al., 2002; de Salas et al., 2011). Moreover, it is worth noting that *P-n. heimii*, together with other large diatoms (e.g. *Thalassiothrix antarctica*, *Proboscia alata*), have been reported to be major contributors of a Subsurface Chlorophyll Maximum (SCM) consistently observed between 53 and 58° S along 140° E (Kopczynska et al., 2001; Parslow et al., 2001). *Navicula directa* also showed maximum abundances at the PFZ site with values ∼5 %. This species has been traditionally described as a benthic-dwelling species (Scott and Marchant, 2005 and references therein) with affinity for sea-ice conditions (Armand, 1997). However, its persistent presence throughout the six-year record and similar seasonal flux pattern to that of other well-known open-ocean species of the ACC, such as *Thalassiosira gracilis* group ($r = 0.8$, $n = 108$; Fig. 5b) point to a pelagic distribution of this species. This concept agrees well with Kopczynska et al. (1986) and Waite and Nodder (2001) who documented *Navicula* populations of considerable abundance in areas remote from coastal and sea-ice influence in the Australian sector.

Although in many aspects the composition of the diatom assemblage at the 61° S site was similar to that of station 54° S, there were some qualitative and quantitative difference. As a result of the southward increase in the abundance of *F. kerguelensis*, the diversity (H') and the relative contribution of most of the secondary constituents of the diatom assemblage at 61° S exhibited lower values than at 54° S (Table 4). For example, *Pseudo-nitzchia* species that represented cumulatively 13 % of the integrated assemblage, dropped to < 1 % at the 61° S site. *Navicula directa* followed a similar pattern with maximum abundances at 54° S (5 %) and negligible fluxes at 61° S. It is possible however, that other factors, such as selective grazing or ecological constraints may also account for the lower contribution of these species in the AZ. Moreover, the sea-ice affiliated species *Fragilariopsis curta* and *Fragilariopsis cylindrus*, that contributed significantly to total diatom fluxes at station 61° S during limited intervals (up to 4 and 3 % during summer; Rigual-Hernández et al., 2015), exhibited negligible fluxes at the 54° S site, which reflects the absence of sea-ice influence in the PFZ south of Tasmania.

BGD
12, 8615–8690, 2015

5.3 Seasonal variability of diatom assemblages

Variations in the magnitude of particulate fluxes at the 47 and 54° S sites are primarily driven by the seasonal cycle of primary production. Low chlorophyll *a* concentrations and particle fluxes over winter are consistent with light limited production in response to reduced incident radiation and mixed layer deepening. The duration of biomass accumulation extends from November to March in the SAZ and has a short weak maximum from November to January in the PFZ (Figs. 2a and 3a; Bowie et al., 2011a). The period of enhanced particle export was broadly in line with the chlorophyll *a* estimates at both sites. Taking into account that diatoms are, by far, the main contributors to the biogenic silica production at the 54° S site, and that the biogenic silica fraction, in turn, dominated the total mass flux, the strong correlation between diatom valve and mass fluxes ($r = 0.85$; $n = 88$) suggests that the particle export at the PFZ is mainly mediated by diatoms. In contrast, at the 47° S site, the silica-poor content of the particles and the low correlation between diatom valve and mass fluxes ($r = 0.37$; $n = 30$) indicates a minor role for diatoms in regulating the export in the SAZ. These results underscore the contrasting role that diatoms play in the controls on the flux north and south the SAF (Trull et al., 2001a; Ebersbach et al., 2011).

The annual export maxima of total mass and diatom valve flux at 54° S were separated into two peaks for most of the years (Figs. 5a and 7). A similar double peak feature of the particle bloom has been previously reported in the APZ and AZ of the southwest Pacific (Honjo et al., 2000; Grigorov et al., 2014) and in the APZ of the south Atlantic (Fischer et al., 2002). Honjo (2004) speculated that such a double peak structure may be due to a break in primary production caused by a temporary depletion of macro- or micronutrients followed by a rapid replenishment of the limiting nutrient(s). Grigorov et al. (2014) attributed a drop in the diatom flux between two periods of enhanced diatom export to a strong storm event that mixed the diatom biomass out of the surface layer. The lack of accompanying in situ measurements of nutrient concentration and mixed layer depth precludes the direct assessment of these possibilities. Ecological factors

BGD
12, 8615–8690, 2015

might also play a role, for example the seasonal increase in trophic complexity may increase mesopelagic particle remineralization rates above the traps (Wassmann, 1998). Statistical funnel (i.e. the spatial domain containing the likely origins for collected sinking particles) issues related to non-uniform surface fields (Siegel and Deuser, 1997) are possible, but seem unlikely (Hamilton, 2006) based on the sparse available ocean colour observations (admittedly quite limited by cloud cover).

The initial diatom population size (i.e. seeding stock), species-specific physiological traits and selective grazing pressure are crucial factors determining which diatom species dominates or co-dominate an individual bloom (Assmy et al., 2007; Assmy et al., 2013; Boyd, 2013). The chain-forming *F. kerguelensis* is one of the most abundant diatom species in the iron-limited waters of the ACC (e.g. Hart, 1934; Hasle, 1969; Laubscher et al., 1993; Bathmann et al., 1997; Smetacek et al., 2002) and has been reported to represent up to 90 % of the summer diatom populations in the Australian sector south of the Polar Front (PF; Gall et al., 2001). The high relative contribution of *F. kerguelensis* throughout our six-year time series is consistent with these latter studies and suggests the presence of a large seeding population of this species before the onset of the diatom bloom. These large initial seed stocks, together with the effective mechanical protection of its robust frustule (Hamm et al., 2003) against the heavy copepod grazing pressure of the ACC (Pollard et al., 2002; McLeod et al., 2010) are most likely the main factors determining the dominance of *F. kerguelensis* during the growth season. The increase in the relative abundance of the lightly-silicified *Pseudo-nitzschia* cf. *lineola* and small *Fragilariopsis* species during the second part of the bloom (Figs. 5b and 7) is consistent with the observations of .Kopczynska et al. (2001) who reported *Fragilariopsis pseudonana* and *Pseudo-nitzschia lineola* dominating the diatom assemblages in the iron-limited waters of the PFZ south of Tasmania during late summer. Assmy et al. (2007) reported large numbers of *P-n. lineola* during the last stages of the fertilization experiment EisenEx in Atlantic Sector of the Southern Ocean, indicating the capacity of this diatom to outcompete other taxa under iron-limiting conditions. Moreover, small *Fragilariopsis* and *Pseudo-nitzschia* species are known to pro-

BGD
12, 8615–8690, 2015

duce an iron-storage protein (ferritin) that allow them to undergo more cell divisions than other open-ocean diatoms under low iron concentrations (Marchetti et al., 2009). We speculate, that due to these particular physiological traits *Pseudo-nitzschia* and small-*Fragilariopsis* species may gain a competitive advantage under the environmental conditions during the last stages of the diatom bloom (i.e. low-silica and iron-limiting concentrations, and enhanced PAR levels) enabling such species to escape grazing and/or outcompete other diatoms. However, this scenario does not account for our observations in 2002–2003, when *Pseudo-nitzschia* and small-*Fragilariopsis* species exhibited higher relative contribution to the in the first seasonal export peak (Figs. 5b and 7). This exceptional seasonal export peak remained unexplained and likely due to other environmental conditions not captured by our study.

Maximum annual relative contribution of *Pseudo-nitzschia hemii*, the *Proboscia* group and *Thalassiothrix antarctica* were often registered between the end of the growth season and winter (Fig. 5b). As previously noted, high numbers of these species have been found in association to a subsurface chlorophyll maximum in this region during summer and autumn (Kopczynska et al., 2001; Parslow et al., 2001). We suggest that the intensification of the convective mixing and the decrease in light during this period could have led to the sedimentation of these deep-dwellers following the conceptual scheme for the seasonal development of planktonic communities in the PFZ and POOZ (Permanently Open Ocean Zone) suggested by Quéguiner (2013).

The less defined seasonal pattern and lower amplitude of the diatom fluxes observed at the 47° S site (Fig. 4) are a reflection of the different algal community north of the SAF, dominated by non-siliceous taxa with lower abundances of diatoms (Odate and Fukuchi, 1995; Kopczynska et al., 2001; de Salas et al., 2011). For both years of our study, the highest annual diatom export events coincided with the onset of the biomass accumulation in the surface waters, indicating that diatoms responded rapidly to the enhanced light levels (Fig. 2a) and to the formation of a stable and shallow mixed layer (Rintoul and Trull, 2001). However, unlike the chlorophyll *a* concentration that gradually increased throughout the spring, diatom export rapidly returned to winter values

BGD
12, 8615–8690, 2015

most likely caused by the depletion of the winter silicate and/or iron stocks (Lannuzel et al., 2011). This seasonal pattern is characteristic of the SAZ and other silicate-poor environments at lower latitudes, where diatoms typically bloom at the beginning of the successional sequence and then are replaced by other functional groups such as *Phaeocystis*, coccolithophores and dinoflagellates (e.g. Margalef, 1978; Thunell et al., 1996; Balch, 2004; Alvain et al., 2008; Rigual-Hernández et al., 2013). The increase in the diatom and BSi fluxes from January to early March 2001 suggests the export of a second diatom bloom that year. South of Tasmania the SAZ exhibits a complex physical structure with frequent wind mixing events (Yuan, 2004) and fronts meandering and forming eddies that can reach the trap location (Rintoul and Trull, 2001; Herraiz-Borreguero and Rintoul, 2011). Thus, it is likely that any of these mechanisms injected nutrients into the surface layer of the 47° S site fuelling diatom production and allowing the "reset" of phytoplankton succession. This concept would also explain the second peak of chlorophyll *a* registered during mid-late summer that year (Fig. 2a).

In terms of population dynamics, the seasonal succession of species at the 47° S site was not as clearly expressed as in station 54° S and none of the diatom species seem to play an important role in the export controls of any of the components of the flux as indicated by the results of the PCA (Fig. 6a). *Fragilariopsis kerguelensis* exhibited fairly constant relative abundances throughout the record suggesting little competition for resources with other diatom species. The temperate-to-warm water species *Hemidiscus cuneiformis* and *Azpeitia tabularis* (Romero et al., 2005; Romero et al., 2015) showed their maximum contribution at times of maximum diatom export which suggests that these species are the first to respond to nutrient supply in the surface waters in this region. Moreover, highest relative contribution of the oligotrophic *N. bicapitata* (Romero et al., 2000) registered during periods of low productivity indicates the capacity of this species to maintain relatively constant stocks in the surface waters year-round.

BGD
12, 8615–8690, 2015

5.4 Ecological flux vectors in the PFZ

The short and vigorous summer particle export, consistently observed during our six year record at the 54° S trap is characteristic of high latitude systems (e.g. Honjo et al., 2000; Fischer et al., 2002; Pilskaln et al., 2004) and can contribute up to 66 % of the annual POC export to 800 m in just two months (e.g. year 1999–2000). Therefore, these large summer pulses of POC are responsible for a major proportion of the variability in carbon sequestration from the atmosphere in the PFZ. The mechanism is primarily through the increase in the overall flux, because the fractional POC content was not observed to increase during high flux periods. For example, % POC for year 1999-2000 ranged between 1.2 and 3.7 %, and maximum relative abundances occurred at times of relatively low fluxes (Fig. 3b).

The strong positive correlation between Factor 1 and POC fluxes at the 54° S site (Table 6) indicates an intimate association between high relative abundances of the "High-export group" species and pulses of POC export. As a specific example of this, during January 1999 and December 2000, when the highest contribution of "High-export group" was noted (55–60 % of the total diatom flux; Fig 7), the PFZ sediment trap registered the largest POC fluxes of the record (up to 23 mg m^{-2} d^{-1}; Fig. 7). Interestingly, these observations of elevated POC flux coincide with significantly lower summer sea surface temperatures than other years.

All the members of the "High-export group" have been previously reported as important components of both natural and iron-fertilized blooms in the Southern Ocean (Bathmann et al., 1997; Bracher et al., 1999; Waite and Nodder, 2001; Smetacek et al., 2002; Assmy et al., 2007; Quéguiner, 2013; Grigorov et al., 2014; Sackett et al., 2014; Rigual-Hernández et al., 2015). The increase in the relative abundance and fluxes of these species during the growth season indicates that they respond opportunistically to the enhanced light levels, most likely undergoing cycles of rapid biomass buildup followed by mass mortality and sinking in the form of aggregates (Smetacek et al., 2004; Green and Sambrotto, 2006; Assmy et al., 2013; Quéguiner, 2013; Grigorov et al.,

BGD
12, 8615–8690, 2015

2014). This concept is supported by the recent findings of (Closset et al., under review) who documented an increase in the particle sinking speeds at the 54° S site during the summer 1999-2000 of up to at least 35 m d^{-1}, a value that falls within the range of previous estimates for marine snow sinking rates (Turner, 2002; Trull et al., 2008; Laurenceau et al., 2014). Moreover, other regionally-relevant PFZ studies (Ebersbach et al., 2011; Grigorov et al., 2014) concluded that aggregates are the principal form of particle export during the growth season. Taken together, our data and these studies strongly suggest that aggregate formation is a widespread mechanism of the summer bloom in the open-ocean waters of the ACC.

The aggregation and sedimentation of particles during a phytoplankton bloom is determined by the complex interaction of several factors including, the composition of the phytoplankton assemblage, biomass and particle accumulation, secretion of transparent exopolymer particles (TEP) and packaging by the zooplankton community (Passow, 2002; Turner, 2002; Grossart et al., 2006; Boyd and Trull, 2007; Burd and Jackson, 2009; Iversen and Ploug, 2010). We suggest that the massive development of "High-export group" diatoms during the growth season facilitates the formation of aggregates in the upper water column, which results in an increase in sinking rates and POC fluxes. Aggregates, and particularly diatom flocs, are rich in exopolymers that increase their effectiveness at scavenging particles they have collided with (Alldredge and McGillivary, 1991; Passow and De La Rocha, 2006). Therefore, it is possible that that the formation of aggregates during the diatom bloom facilitated the scavenging of other particles (including phytoplankton chains and cells, biominerals and detritus), leading to the co-sedimentation of the major components of the flux (i.e. calcium carbonate, silica and organic carbon). This scavenging mechanism is consistent with previous laboratory observations made by Passow and De La Rocha (2006) and can explain the increase of the sinking rates during the growth season as well as the positive correlation between Factor 1 and all bulk components of the flux (Fig. 6b; Table 6b).

Since most of the members of "High-export group" are of relatively small size and weakly silicified, it is unlikely that these species accounted for the major fraction of the

BGD
12, 8615–8690, 2015

BSi export during the summer bloom for most of the years. In contrast, the large and thick-shelled *F. kerguelensis* is a more compelling candidate tow be responsible for the bulk of the BSi export, because despite the fact that its lowest relative abundance always occurred during the productive season, it often represented more than 50 % of the summer assemblage (Fig. 5b). In terms of carbonate export, the correlation between Factor 1 and carbonate flux is not as strong as with the rest of the components of the flux but still high (Fig. 6b; Table 6b), indicating that highest relative contribution of the "High-export group" diatoms is also associated with high carbonate export. It is possible that that the formation of aggregates during the diatom bloom also facilitated the scavenging of at least the fine fraction of the carbonate (mainly coccoliths; Ziveri et al., 2007; Iversen and Ploug, 2010) which would have led to the co-sedimentation of the BSi, POC and carbonate fractions. However, other seasonal ecological influences are also likely to be involved, given that the contribution of larger carbonate particles in the form of foraminifera tests is also increased in summer (King and Howard, 2003).

In regard to the autumn and winter months, the low particle fluxes observed during this period were overwhelmingly dominated by *F. kerguelensis* (up to 97 % of the diatom assemblage) and characterized by very low settling speeds (up to less than 3 m d^{-1}; Closset et al., 2015). These observations are consistent with the findings of Grigorov et al. (2014) who reported that diatom export outside the productive period in the pelagic waters of the ACC mainly occurs in the form of single cells and chains. Small and slow sinking particles are more exposed to degradation processes (e.g. silica dissolution, bacterial remineralization) during settlement than larger and rapid-sinking aggregates (Trull et al., 2008). Therefore, the enrichment of the dissolution-resistant *F. kerguelensis* during this period is most likely related to the enhanced, selective dissolution of more lightly-silicified species during the non-productive season.

5.5 Relative importance of the SAZ and PFZ to carbon export

The depth at which the organic carbon is remineralized to CO_2 by zooplankton and bacteria determines the timescales during which carbon is sequestered from the at-

BGD
12, 8615–8690, 2015

mosphere (Yamanaka and Tajika, 1996; Smetacek et al., 2012). In the SAZ and the PFZ, the fraction of organic carbon recycled within the winter mixed layer (> 400 m in the SAZ and between 150–200 m in the PFZ; Rintoul and Bullister, 1999; Rintoul and Trull, 2001) would reequilibrate with the atmosphere within months, whereas only the comparatively smaller portion that reaches deeper layers will remain in the ocean interior for centuries or longer timescales (Trull et al., 2001a). Thus, from the perspective of carbon sequestration, the POC fluxes measured by the traps reported in this study are probably of greater importance than those remineralized at mid-depths.

Despite the fact that total mass fluxes in the PFZ at ~ 1 km were two-fold larger than those of the SAZ, the annual POC export was almost identical in both regions (Fig. 8a), implying that particles sinking out the mixed layer in the SAZ were relatively POC rich (Trull et al., 2001a; Ebersbach et al., 2011). Taking into account that gross primary production is similar in the two zones, or perhaps somewhat lower in the PFZ (Fig. 8b; Lourey and Trull, 2001; Cavagna et al., 2011; Westwood et al., 2011), our results challenge the notion that for a given similar level of production, diatom-dominated ecosystems export greater amounts of carbon to the deep ocean than ecosystems dominated by smaller, non-siliceous phytoplankton (Buesseler, 1998; Boyd and Newton, 1999; Laws et al., 2000). Trull et al. (2001) hypothesised that the similar POC export at both sites could be due to either (1) a more efficient repackaging of carbon for deep transport by the zooplankton community in the SAZ than in the PFZ or (2) to the fact that the silicate-rich particles exported in the PFZ may experience stronger loses of organic carbon at mesopelagic depths than do the carbonate-rich particles of the SAZ. Results from of the SAZ-sense programme (Bowie et al., 2011b) taken together with the data presented in this study provide key information to assess these hypotheses.

Analysis of the flux size spectra at the 47 and 54° S sites by Ebersbach et al. (2011) during January and February 2007 revealed that the vertical export at both stations was dominated by heavily processed particles, mainly faecal aggregates with a slight shift towards smaller particles within the PFZ due to abundant chains of diatoms sinking

BGD
12, 8615–8690, 2015

individually or as part of unconsolidated aggregates. Although the latter study was limited to a short observational period, the results of Ebersbach et al. (2011) suggest that zooplankton grazing had a similar impact on the control of particle export at both sites, and therefore the first hypothesis seems unlikely.

On the other hand, our data shows that only a few diatom species, particularly *F. kerguelensis*, dominate the particle export in the silicate-rich and iron-limited waters of the PFZ and AZ. Most of these species are known to significantly increase their BSi : PON and BSi : POC ratios under iron deficiency resulting in the thickening of its already robust frustule (Takeda, 1998; Hoffmann et al., 2007). Furthermore, recent findings from the European Iron Fertilization Experiment (EIFEX; Smetacek et al., 2012) illustrated that the cellular content of a large fraction of the *F. kerguelensis* stock outside and inside the patch was recycled in the surface layer, resulting in the disproportional sinking of empty frustules to the deep ocean (Assmy et al., 2013). The former authors concluded that due to these particular traits, *F. kerguelensis* and other exceptionally robust diatoms, such as *Thalassiosira lentiginosa*, *Thalassionema nitzschioides* and *Thalassiothrix antarctica* preferentially sequester silicon relative to carbon in the iron-limited waters of the ACC. This concept is consistent with our findings in the open-waters of the Australian sector south of the SAF, and would help to explain the low POC content and POC : BSi ratios of the particles registered at meso- and bathypelagic depths by our PFZ and AZ traps.

Significantly, comparisons of our results (Fig. 8a) with satellite and in-situ measurements of primary production (Fig. 8b) suggest that high BSi sedimentation rates should be interpreted as a proxy for iron-limited diatom assemblages (Hutchins and Bruland, 1998; Takeda, 1998; Assmy et al., 2013) rather than for high primary production. This conclusion raises corresponding caution to previous studies that suggest that higher Si fluxes in the past refer to a stronger biological carbon pump (Anderson et al., 2009; Sigman et al., 2010).

BGD
12, 8615–8690, 2015

6 Conclusions

This study reports on the chemical (biogenic silica, carbonate and POC) and biological (diatoms) composition of material exported at ~ 1 km depth at two sites representative of two major hydrological regions of the Australian sector of the Southern Ocean, the SAZ and PFZ. As a result of different algal communities, the composition and magnitude of the sinking particle fluxes was very different between sites, with higher and biogenic silicate-dominated fluxes in the PFZ versus lower and carbonate-dominated fluxes in the SAZ. Despite these differences, the POC export reaching the traps was indistinguishable between sites (~ 1 g m^{-2} yr^{-1}). Seasonality and flux magnitude was more pronounced in the PFZ. The vigorous settling of biogenic particles during summer in the PFZ accounted for a large fraction of the annual POC export. These summer pulses are a major factor responsible for the variability in carbon sequestration from the atmosphere in this region. Our results suggest that the development of a group of bloom-forming diatom species during the growth season lead to the formation of algal and/or faecal aggregates. The production and sinking of these aggregates most likely facilitated the scavenging of other particles in the water column, and thus the co-sedimentation of the all the components of the flux. *Fragilariopsis kerguelensis* dominated the diatom sinking assemblage at both sites and was considered the major biological vector decoupling the carbon and silicon cycles in the waters south the SAF. Comparisons of our data with in-situ and satellite primary production estimates lead us to conclude that high biogenic silica accumulation rates in the sedimentary record should be interpreted as a proxy for iron-limited diatom assemblages rather than for a stronger biological pump.

Acknowledgements. The SAZ Project sediment trap moorings have received support from many sources, including Australian Antarctic Sciences awards AAS1156 and AA2256 (T. Trull), the US National Science Foundation Office of Polar Programs (R. Francois, T. Trull, S. Honjo and S. Manganini), the Belgian Science and Policy Office (F. Dehairs), CSIRO Marine Laboratories, and the Australian Integrated Marine Observing System (of which they are currently a component of the IMOS Southern Ocean Time Series Facility; www.imos.org.au). This work

BGD
12, 8615–8690, 2015

was made possible by the Australian Government's Australian Antarctic Science Grant Program (Project number 4078) and Macquarie University (A. Rigual-Hernández and L. Armand). The chlorophyll *a* and PAR data sets and chlorophyll *a* visualizations used in this paper were produced with the Giovanni online data system, developed and maintained by the NASA GES DISC. Primary productivity estimates were made available by the Ocean Productivity website (http://www.science.oregonstate.edu/ocean.productivity/). Diana M. Davies is thanked for performing biogeochemical analyses on the trap material. Anne-Marie Ballegeer is acknowledged for her technical support in the preparation of samples and comments on an early draft of the manuscript. Thanks to Jan Lieser and John Baumgartner for their assistance in the remote sensing analysis. The authors are thankful to Jessica Wilks and Kelly Lawler for their help in the microscopy analysis and taxonomic identifications. The authors acknowledge the assistance and support of Nicole Vella and Debra Birch from the Macquarie University Microscopy Unit in the scanning electron microscopy analysis.

References

Abrantes, F.: Diatom assemblages as upwelling indicators in surface sediments off Portugal, Mar. Geol., 85, 15–39, 1988.

Acker, J. G. and Leptoukh, G.: Online Analysis Enhances Use of NASA Earth Science Data, Eos, Transactions, AGU, 88, 14–17, 2007.

Alldredge, A. L. and McGillivary, P.: The attachment probabilities of marine snow and their implications for particle coagulation in the ocean, Deep-Sea Res., 38, 431–443, 1991.

Alvain, S., Moulin, C., Dandonneau, Y., and Bréon, F. M.: Remote sensing of phytoplankton groups in case 1 waters from global SeaWiFS imagery, Deep-Sea Res. Pt. I, 52, 1989–2004, 2005.

Alvain, S., Moulin, C., Dandonneau, Y., and Loisel, H.: Seasonal distribution and succession of dominant phytoplankton groups in the global ocean: A satellite view, Global Biogeochem. Cy., 22, GB3001, doi:10.1029/2007GB003154, 2008.

Alvain, S., Le Quéré, C., Bopp, L., Racault, M.-F., Beaugrand, G., Dessailly, D., and Buitenhuis, E. T.: Rapid climatic driven shifts of diatoms at high latitudes, Remote Sens. Environ., 132, 195–201, 2013.

BGD
12, 8615–8690, 2015

Anderson, R. F., Chase, Z., Fleisher, M. Q., and Sachs, J.: The Southern Ocean's biological pump during the Last Glacial Maximum, Deep-Sea Res. Pt. II, 49, 1909–1938, 2002.
Anderson, R. F., Ali, S., Bradtmiller, L. I., Nielsen, S. H. H., Fleisher, M. Q., Anderson, B. E., and Burckle, L. H.: Wind-Driven Upwelling in the Southern Ocean and the Deglacial Rise in Atmospheric CO_2, Science, 323, 1443–1448, 2009.
Armand, L. K., Crosta, X., Romero, O., and Pichon, J.-J.: The biogeography of major diatom taxa in Southern Ocean sediments: 1. Sea ice related species, Palaeogeogr. Palaeoecol., 223, 93–126, 2005.
Armand, L. K. A.: The use of diatom transfer functions in estimating sea-surface temperature and sea-ice in cores from the southeast Indian Ocean, PhD, Australian National University, Canberra, Australia, 392 pp., 1997.
Arrigo, K. R. and van Dijken, G. L.: Phytoplankton dynamics within 37 Antarctic coastal polynya systems, J. Geophys. Res.-Oceans, 108, 3271, doi:10.1029/2002JC001739, 2003.
Arrigo, K. R., Worthen, D., Schnell, A., and Lizotte, M. P.: Primary production in Southern Ocean waters, J. Geophys. Res.-Oceans, 103, 15587–15600, 1998.
Arrigo, K. R., van Dijken, G. L., and Bushinsky, S.: Primary production in the Southern Ocean, 1997–2006, J. Geophys. Res.-Oceans, 113, C08004, doi:10.1029/2007JC004551, 2008.
Assmy, P., Henjes, J., Klaas, C., and Smetacek, V.: Mechanisms determining species dominance in a phytoplankton bloom induced by the iron fertilization experiment EisenEx in the Southern Ocean, Deep-Sea Res. Pt. I, 54, 340–362, 2007.
Assmy, P., Smetacek, V., Montresor, M., Klaas, C., Henjes, J., Strass, V. H., Arrieta, J. M., Bathmann, U., Berg, G. M., Breitbarth, E., Cisewski, B., Friedrichs, L., Fuchs, N., Herndl, G. J., Jansen, S., Krägefsky, S., Latasa, M., Peeken, I., Röttgers, R., Scharek, R., Schüller, S. E., Steigenberger, S., Webb, A., and Wolf-Gladrow, D.: Thick-shelled, grazer-protected diatoms decouple ocean carbon and silicon cycles in the iron-limited Antarctic Circumpolar Current, P. Natl. Acad. Sci., 110, 20633–20638, 2013.
Baker, E. T., Milburn, H. B., and Tennant, D. A.: Field assessment of sediment trap efficiency under varying flow conditions, J. Mar. Res., 46, 573–592, 1988.
Balch, W. M.: Re-evaluation of the physiological ecology of coccolithophores, in: Coccolithophores. From Molecular Processes to Global Impact, edited by: Thierstein, H. R. and Young, J. R., Springer-Verlag, Berlin, 165–190, 2004.
Bárcena, M. A. and Abrantes, F.: Evidence of a high-productivity area off the coast of Málaga from studies of diatoms in surface sediments, Mar. Micropaleontol., 35, 91–103, 1998.

BGD
12, 8615–8690, 2015

Barker, S., Diz, P., Vautravers, M. J., Pike, J., Knorr, G., Hall, I. R., and Broecker, W. S.: Interhemispheric Atlantic seesaw response during the last deglaciation, Nature, 457, 1097–1102, 2009.

Bathmann, U. V., Scharek, R., Klaas, C., Dubischar, C. D., and Smetacek, V.: Spring development of phytoplankton biomass and composition in major water masses of the Atlantic sector of the Southern Ocean, Deep-Sea Res. Pt. II, 44, 51–67, 1997.

Behrenfeld, M. J. and Falkowski, P. G.: Photosynthetic rates derived from satellite-based chlorophyll concentration, Limnol. Oceanogr., 42, 1–20, 1997.

Behrenfeld, M. J., Boss, E., Siegel, D. A., and Shea, D. M.: Carbon-based ocean productivity and phytoplankton physiology from space, Global Biogeochem. Cy., 19, GB1006, doi:10.1029/2004GB002299, 2005.

Bishop, J. K. B. and Rossow, W. B.: Spatial and temporal variability of global surface solar irradiance, J. Geophys. Res.-Oceans, 96, 16839–16858, 1991.

Blain, S., Tréguer, P., Belviso, S., Bucciarelli, E., Denis, M., Desabre, S., Fiala, M., Martin Jézéquel, V., Le Fèvre, J., Mayzaud, P., Marty, J.-C., and Razouls, S.: A biogeochemical study of the island mass effect in the context of the iron hypothesis: Kerguelen Islands, Southern Ocean, Deep-Sea Res. Pt. I, 48, 163–187, 2001.

Bowie, A. R., Lannuzel, D., Remenyi, T. A., Wagener, T., Lam, P. J., Boyd, P. W., Guieu, C., Townsend, A. T., and Trull, T. W.: Biogeochemical iron budgets of the Southern Ocean south of Australia: Decoupling of iron and nutrient cycles in the subantarctic zone by the summertime supply, Global Biogeochem. Cy., 23, GB4034, doi:10.1029/2009GB003500, 2009.

Bowie, A. R., Brian Griffiths, F., Dehairs, F., and Trull, T.: Oceanography of the subantarctic and Polar Frontal Zones south of Australia during summer: Setting for the SAZ-Sense study, Deep-Sea Res. Pt. II, 58, 2059–2070, 2011a.

Bowie, A. R., Trull, T. W., and Dehairs, F.: Estimating the sensitivity of the subantarctic zone to environmental change: The SAZ-Sense project, Deep-Sea Res. Pt. II, 58, 2051–2058, 2011b.

Boyd, P. W.: Environmental factors controlling phytoplankton processes in the Southern Ocean, J. Phycol., 38, 844–861, 2002.

Boyd, P. W.: Diatom traits regulate Southern Ocean silica leakage, P. Natl. Acad. Sci., 110, 20358–20359, 2013.

BGD
12, 8615–8690, 2015

Boyd, P. W. and Newton, P. P.: Does planktonic community structure determine downward particulate organic carbon flux in different oceanic provinces?, Deep-Sea Res. Pt. I, 46, 63–91, 1999.
Boyd, P. W. and Trull, T. W.: Understanding the export of biogenic particles in oceanic waters: Is there consensus?, Prog. Oceanogr., 72, 276–312, 2007.
Boyd, P. W., LaRoche, J., Gall, M. P., Frew, R., and McKay, R. M. L.: Role of iron, light, and silicate in controlling algal biomass in subantarctic waters SE of New Zealand, J. Geophys. Res.-Oceans, 104, 13395–13408, 1999.
Boyd, P. W., Crossley, A. C., DiTullio, G. R., Griffiths, F. B., Hutchins, D. A., Queguiner, B., Sedwick, P. N., and Trull, T. W.: Control of phytoplankton growth by iron supply and irradiance in the subantarctic Southern Ocean: Experimental results from the SAZ Project, J. Geophys. Res.-Oceans, 106, 31573–31583, 2001.
Boyd, P. W., Jickells, T., Law, C. S., Blain, S., Boyle, E. A., Buesseler, K. O., Coale, K. H., Cullen, J. J., de Baar, H. J. W., Follows, M., Harvey, M., Lancelot, C., Levasseur, M., Owens, N. P. J., Pollard, R., Rivkin, R. B., Sarmiento, J., Schoemann, V., Smetacek, V., Takeda, S., Tsuda, A., Turner, S., and Watson, A. J.: Mesoscale Iron Enrichment Experiments 1993–2005: Synthesis and Future Directions, Science, 315, 612–617, 2007.
Boyd, P. W., Strzepek, R., Fu, F., and Hutchins, D. A.: Environmental control of open-ocean phytoplankton groups: Now and in the future, Limnol. Oceanogr., 55, 1353–1376, 2010.
Bracher, A., Kroon, B., and Lucas, M.: Primary production, physiological state and composition of phytoplankton in the Atlantic sector ot the Southern Ocean, Mar. Ecol.-Progr. Ser., 190, 1–16, 1999.
Bray, S., Trull, T. W., and Manganini, S.: SAZ Project Moored Sediment Traps: Results of the 1997–1998 Deployments, Antarctic Cooperative Research Centre, Hobart, Tasmania, Australia, 128 pp., 2000.
Brzezinski, M. A., Nelson, D. M., Franck, V. M., and Sigmon, D. E.: Silicon dynamics within an intense open-ocean diatom bloom in the Pacific sector of the Southern Ocean, Deep-Sea Res. Pt. II, 48, 3997–4018, 2001.
Brzezinski, M. A., Pride, C. J., Franck, V. M., Sigman, D. M., Sarmiento, J. L., Matsumoto, K., Gruber, N., Rau, G. H., and Coale, K. H.: A switch from Si(OH)4 to NO3- depletion in the glacial Southern Ocean, Geophys. Res. Lett., 29, 5-1–5-4, 2002.
Buesseler, K. O.: The decoupling of production and particulate export in the surface ocean, Global Biogeochem. Cy., 12, 297–310, 1998.

BGD
12, 8615–8690, 2015

Buesseler, K. O., Ball, L., Andrews, J., Cochran, J. K., Hirschberg, D. J., Bacon, M. P., Fleer, A., and Brzezinski, M.: Upper ocean export of particulate organic carbon and biogenic silica in the Southern Ocean along 170° W, Deep-Sea Res. Pt. II, 48, 4275–4297, 2001.

Buesseler, K. O., Antia, A. N., Chen, M., Fowler, S. W., Gardner, W. D., Gustafsson, O., Harada, K., Michaels, A. F., der Loeff, M. R. v., and Sarin, M.: An assessment of the use of sediment traps for estimating upper ocean particle fuxes, J. Mar. Res., 65, 345–416, 2007.

Burckle, L. H. and Cirilli, J.: Origin of Diatom Ooze Belt in the Southern Ocean: Implications for Late Quaternary Paleoceanography, Micropaleontology, 33, 82–86, 1987.

Burd, A. B. and Jackson, G. A.: Particle aggregation, Annu. Rev. Mar. Sci., 1, 65–90, 2009.

Cavagna, A.-J., Elskens, M., Griffiths, F. B., Fripiat, F., Jacquet, S. H. M., Westwood, K. J., and Dehairs, F.: Contrasting regimes of production and potential for carbon export in the Sub-Antarctic and Polar Frontal Zones south of Tasmania, Deep-Sea Res. Pt. II, 58, 2235–2247, 2011.

Closset, I., Cardinal, D., Bray, S., Thil, F., Djouraev, I., Rigual-Hernández, A. S., and Trull, T. W.: Seasonal variations, origin and fate of settling diatoms in the Southern Ocean tracked by silicon isotope records in deep sediment traps, Global Biogeochem. Cy., under review, 2015.

Crosta, X., Pichon, J.-J., and Labracherie, M.: Distribution of Chaetoceros resting spores in modern peri-Antarctic sediments, Mar. Micropaleontol., 29, 283–299, 1997.

Crosta, X., Romero, O., Armand, L. K., and Pichon, J.-J.: The biogeography of major diatom taxa in Southern Ocean sediments: 2. Open ocean related species, Palaeogeogr. Palaeoecol., 223, 66–92, 2005.

de Baar, H. J. W., de Jong, J. T. M., Bakker, D. C. E., Loscher, B. M., Veth, C., Bathmann, U., and Smetacek, V.: Importance of iron for plankton blooms and carbon dioxide drawdown in the Southern Ocean, Nature, 373, 412–415, 1995.

De La Rocha, C.: The biological pump, in: Geochemistry of Earth Surface Systems: A derivative of the Treatise on Geochemistry, edited by: Holland, H. D. and Turekian, K. K., Academic Press, 425 pp., 2010.

de Salas, M. F., Eriksen, R., Davidson, A. T., and Wright, S. W.: Protistan communities in the Australian sector of the Sub-Antarctic Zone during SAZ-Sense, Deep-Sea Res. Pt. II, 58, 2135–2149, 2011.

Deacon, G. E. R.: Physical and biological zonation in the Southern Ocean, Deep-Sea Res., 29, 1–15, 1982.

BGD
12, 8615–8690, 2015

DeMaster, D. J.: The supply and accumulation of silica in the marine environment, Geochim. Cosmochim. Ac., 45, 1715–1732, 1981.
DeMaster, D. J.: The accumulation and cycling of biogenic silica in the Southern Ocean: revisiting the marine silica budget, Deep-Sea Res. Pt. II, 49, 3155–3167, 2002.
Downes, S. M., Bindoff, N. L., and Rintoul, S. R.: Impacts of Climate Change on the Subduction of Mode and Intermediate Water Masses in the Southern Ocean, J. Climate, 22, 3289–3302, 2009.
Ebersbach, F., Trull, T. W., Davies, D. M., and Bray, S. G.: Controls on mesopelagic particle fluxes in the Sub-Antarctic and Polar Frontal Zones in the Southern Ocean south of Australia in summer – Perspectives from free-drifting sediment traps, Deep-Sea Res. Pt. II, 58, 2260–2276, 2011.
Esper, O., Gersonde, R., and Kadagies, N.: Diatom distribution in southeastern Pacific surface sediments and their relationship to modern environmental variables, Palaeogeogr. Palaeoecol., 287, 1–27, 2010.
Falkowski, P. G., Barber, R. T., and Smetacek, V.: Biogeochemical Controls and Feedbacks on Ocean Primary Production, Science, 281, 200–206, 1998.
Fetterer, F., Knowles, K., Meier, W., and Savoie, M.: Sea Ice Index, [Sea Ice Extent], Boulder, Colorado USA: National Snow and Ice Data Center, doi:10.7265/N5QJ7F7W, 2002, updated 2009.
Findlay, C. S. and Giraudeau, J.: Extant calcareous nannoplankton in the Australian Sector of the Southern Ocean (austral summers 1994 and 1995), Mar. Micropaleontol., 40, 417–439, 2000.
Fischer, G., Gersonde, R., and Wefer, G.: Organic carbon, biogenic silica and diatom fluxes in the marginal winter sea-ice zone and in the Polar Front Region: interannual variations and differences in composition, Deep-Sea Res. Pt. II, 49, 1721–1745, 2002.
Fitzwater, S. E., Johnson, K. S., Gordon, R. M., Coale, K. H., and Smith Jr, W. O.: Trace metal concentrations in the Ross Sea and their relationship with nutrients and phytoplankton growth, Deep-Sea Res. Pt. II, 47, 3159–3179, 2000.
Gall, M. P., Boyd, P. W., Hall, J., Safi, K. A., and Chang, H.: Phytoplankton processes, Part 1: Community structure during the Southern Ocean Iron RElease Experiment (SOIREE), Deep-Sea Res. Pt. II, 48, 2551–2570, 2001.

BGD
12, 8615–8690, 2015

Gersonde, R. and Zielinski, U.: The reconstruction of late Quaternary Antarctic sea-ice distribution – the use of diatoms as a proxy for sea-ice, Palaeogeogr. Palaeoecol., 162, 263–286, 2000.
Green, S. E. and Sambrotto, R. N.: Plankton community structure and export of C, N, P and Si in the Antarctic Circumpolar Current, Deep-Sea Res. Pt. II, 53, 620–643, 2006.
Gregg, W. W. and Rousseaux, C. S.: Decadal trends in global pelagic ocean chlorophyll: A new assessment integrating multiple satellites, in situ data, and models, J. Geophys. Res.-Oceans, 119, 5921–5933, 2014.
Grigorov, I., Rigual-Hernandez, A. S., Honjo, S., Kemp, A. E. S., and Armand, L. K.: Settling fluxes of diatoms to the interior of the antarctic circumpolar current along 170° W, Deep-Sea Res. Pt. I, 93, 1–13, 2014.
Grossart, H., Kiørboe, T., Tang, K., Allgaier, M., Yam, E., and Ploug, H.: Interactions between marine snow and heterotrophic bacteria: aggregate formation and microbial dynamics, Aquat. Microb. Ecol., 42, 19–26, 2006.
Gust, G., Byrne, R. H., Bernstein, R. E., Betzer, P. R., and Bowles, W.: Particles fluxes and moving fluids: experience from synchronous trap collection in the Sargassso sea, Deep-Sea Res., 39, 1071–1083, 1992.
Hamilton, K. M.: Evaluating the consistency of satellite and deep sediment trap carbon export data in the Southern Ocean, 2006, Honours thesis, Institute of Antarctic and Southern Ocean Studies, University of Tasmania, Hobart, Tasmania, 151 pp., 2006.
Hamm, C. E., Merkel, R., Springer, O., Jurkojc, P., Maier, C., Prechtel, K., and Smetacek, V.: Architecture and material properties of diatom shells provide effective mechanical protection, Nature, 421, 841–843, 2003.
Hart, T. J.: On the phytoplankton of the south-west Atlantic and the Bellingshausen Sea, 1929–1931, University Press, Discovery Reports, VIII (1934), 1–268, 1934.
Hasle, G. R.: An analysis of the phytoplankton of the Pacific Southern Ocean: abundance, composition and distribution during the Brategg Expedition, 1947–48 Hvalrådets Skr., 52 (1969), 1–168, 1969.
Hasle, G. R. and Syvertsen, E. E.: Marine diatoms, Identifying marine phytoplankton, Academic Press, San Diego, CA, 5–385, 1997.
Hense, I., Bathmann, U. V., and Timmermann, R.: Plankton dynamics in frontal systems of the Southern Ocean, J. Mar. Sys., 27, 235–252, 2000.

BGD
12, 8615–8690, 2015

Herraiz-Borreguero, L. and Rintoul, S. R.: Subantarctic Mode Water variability influenced by mesoscale eddies south of Tasmania, J. Geophys. Res.-Oceans, 115, C04004, doi:10.1029/2008JC005146, 2010.

Herraiz-Borreguero, L. and Rintoul, S. R.: Regional circulation and its impact on upper ocean variability south of Tasmania, Deep-Sea Res. Pt. II, 58, 2071–2081, 2011.

Hirata, T., Hardman-Mountford, N. J., Barlow, R., Lamont, T., Brewin, R., Smyth, T., and Aiken, J.: An inherent optical property approach to the estimation of size-specific photosynthetic rates in eastern boundary upwelling zones from satellite ocean colour: An initial assessment, Prog. Oceanogr., 83, 393–397, 2009.

Hoffmann, L. J., Peeken, I., and Lochte, K.: Effects of iron on the elemental stoichiometry during EIFEX and in the diatoms *Fragilariopsis kerguelensis* and *Chaetoceros dichaeta*, Biogeosciences, 4, 569–579, doi:10.5194/bg-4-569-2007, 2007.

Honjo, S.: Particle export and the biological pump in the Southern Ocean, Antarct. Sci., 16, 501–516, 2004.

Honjo, S., Francois, R., Manganini, S., Dymond, J., and Collier, R.: Particle fluxes to the interior of the Southern Ocean in the Western Pacific sector along 170° W, Deep-Sea Res. Pt. II, 47, 3521–3548, 2000.

Honjo, S., Manganini, S. J., Krishfield, R. A., and Francois, R.: Particulate organic carbon fluxes to the ocean interior and factors controlling the biological pump: A synthesis of global sediment trap programs since 1983, Prog. Oceanogr., 76, 217–285, 2008.

Howard, W. R., Roberts, D., Moy, A. D., Lindsay, M. C. M., Hopcroft, R. R., Trull, T. W., and Bray, S. G.: Distribution, abundance and seasonal flux of pteropods in the Sub-Antarctic Zone, Deep-Sea Res. Pt. II, 58, 2293–2300, 2011.

Hutchins, D. A. and Bruland, K. W.: Iron-limited diatom growth and Si:N uptake ratios in a coastal upwelling regime, Nature, 393, 561–564, 1998.

Iversen, M. H. and Ploug, H.: Ballast minerals and the sinking carbon flux in the ocean: carbon-specific respiration rates and sinking velocity of marine snow aggregates, Biogeosciences, 7, 2613–2624, doi:10.5194/bg-7-2613-2010, 2010.

Johnson, K. S., Gordon, R. M., and Coale, K. H.: What controls dissolved iron concentrations in the world ocean?, Mar. Chem., 57, 137–161, 1997.

King, A. L. and Howard, W. R.: Planktonic foraminiferal flux seasonality in Subantarctic sediment traps: A test for paleoclimate reconstructions, Paleoceanography, 18, 1019, 2003.

BGD
12, 8615–8690, 2015

King, A. L. and Howard, W. R.: $\delta^{18}O$ seasonality of planktonic foraminifera from Southern Ocean sediment traps: Latitudinal gradients and implications for paleoclimate reconstructions, Mar. Micropaleontol., 56, 1–24, 2005.
Kohfeld, K. E., Quéré, C. L., Harrison, S. P., and Anderson, R. F.: Role of Marine Biology in Glacial-Interglacial CO_2 Cycles, Science, 308, 74–78, 2005.
Kopczynska, E. E., Weber, L. H., and El-Sayed, S. Z.: Phytoplankton species composition and abundance in the Indian sector of the Antarctic Ocean, Polar Biol., 6, 161–169, 1986.
Kopczynska, E. E., Dehairs, F., Elskens, M., and Wright, S.: Phytoplankton and microzooplankton variability between the Subtropical and Polar Fronts south of Australia: Thriving under regenerative and new production in late summer, J. Geophys. Res.-Oceans, 106, 31597–31609, 2001.
Kozlova, A.: Diatom algae of the Indian and Pacific sectors of Antarctica, Academy of Sciences of the USSR Institute of Oceanology, Moscow, 1–191, 1966.
Lampitt, R. S. and Antia, A. N.: Particle flux in deep seas: regional characteristics and temporal variability, Deep-Sea Res. Pt. I, 44, 1377–1403, 1997.
Lampitt, R. S., Salter, I., and Johns, D.: Radiolaria: Major exporters of organic carbon to the deep ocean, Global Biogeochem. Cy., 23, GB1010, doi:10.1029/2008GB003221, 2009.
Lannuzel, D., Bowie, A. R., Remenyi, T., Lam, P., Townsend, A., Ibisanmi, E., Butler, E., Wagener, T., and Schoemann, V.: Distributions of dissolved and particulate iron in the sub-Antarctic and Polar Frontal Southern Ocean (Australian sector), Deep-Sea Res. Pt. II, 58, 2094–2112, 2011.
Laubscher, R. K., Perissinotto, R., and McQuaid, C. D.: Phytoplankton production and biomass at frontal zones in the Atlantic sector of the Southern Ocean, Polar Biol., 13, 471–481, 1993.
Laurenceau-Cornec, E. C., Trull, T. W., Davies, D. M., Bray, S. G., Doran, J., Planchon, F., Carlotti, F., Jouandet, M.-P., Cavagna, A.-J., Waite, A. M., and Blain, S.: The relative importance of phytoplankton aggregates and zooplankton fecal pellets to carbon export: insights from free-drifting sediment trap deployments in naturally iron-fertilised waters near the Kerguelen Plateau, Biogeosciences, 12, 1007–1027, doi:10.5194/bg-12-1007-2015, 2015.
Laws, E. A., Falkowski, P. G., Smith, W. O., Ducklow, H., and McCarthy, J. J.: Temperature effects on export production in the open ocean, Global Biogeochem. Cy., 14, 1231–1246, 2000.

BGD
12, 8615–8690, 2015

Ledford-Hoffman, P. A., Demaster, D. J., and Nittrouer, C. A.: Biogenic-silica accumulation in the Ross Sea and the importance of Antarctic continental-shelf deposits in the marine silica budget, Geochim. Cosmochim. Ac., 50, 2099–2110, 1986.
Leventer, A.: Sediment trap diatom assemblages from the northern Antarctic Peninsula region, Deep-Sea Res., 38, 1127–1143, 1991.
Leventer, A. and Dunbar, R. B.: Factors influencing the distribution of diatoms and other algae in the Ross Sea, J. Geophys. Res.-Oceans, 101, 18489–18500, 1996.
Lourey, M. J. and Trull, T. W.: Seasonal nutrient depletion and carbon export in the Subantarctic and Polar Frontal zones of the Southern Ocean south of Australia, J. Geophys. Res.-Oceans, 106, 31463–31487, 2001.
Marchetti, A., Parker, M. S., Moccia, L. P., Lin, E. O., Arrieta, A. L., Ribalet, F., Murphy, M. E. P., Maldonado, M. T., and Armbrust, E. V.: Ferritin is used for iron storage in bloom-forming marine pennate diatoms, Nature, 457, 467–470, 2009.
Margalef, R.: Life-forms of phytoplankton as survival alternatives in an unstable environment, Oceanol. Acta, 1, 493–509, 1978.
Martin, J. H.: Glacial-interglacial CO_2 change: The Iron Hypothesis, Paleoceanography, 5, 1–13, 1990.
Matsumoto, K., Sarmiento, J. L., and Brzezinski, M. A.: Silicic acid leakage from the Southern Ocean: A possible explanation for glacial atmospheric pCO_2, Global Biogeochem. Cy., 16, 5-1–5-23, 2002.
McCartney, M. S.: Subantarctic Mode Water, in: A Voyage of Discovery, edited by: Angel, M. V., Pergamon, New York, 103–119, 1977.
McLeod, D. J., Hosie, G. W., Kitchener, J. A., Takahashi, K. T., and Hunt, B. P. V.: Zooplankton Atlas of the Southern Ocean: The SCAR SO-CPR Survey (1991–2008), Polar Sci., 4, 353–385, 2010.
Mengelt, C., Abbott, M. R., Barth, J. A., Letelier, R. M., Measures, C. I., and Vink, S.: Phytoplankton pigment distribution in relation to silicic acid, iron and the physical structure across the Antarctic Polar Front, 170° W, during austral summer, Deep-Sea Res. Pt. II, 48, 4081–4100, 2001.
Minas, H. and Minas, M.: Net community production in high nutrient-low chlorophyll waters of the tropical and Antarctic Oceans-grazing vs iron hypothesis, Oceanol. Acta, 15, 145–162, 1992.

BGD
12, 8615–8690, 2015

Mongin, M., Matear, R., and Chamberlain, M.: Simulation of chlorophyll and iron supplies in the Sub Antarctic Zone South of Australia, Deep-Sea Res. Pt. II, 58, 2126–2134, 2011.
Moore, J. K. and Abbott, M. R.: Phytoplankton chlorophyll distributions and primary production in the Southern Ocean, J. Geophys. Res.-Oceans, 105, 28709–28722, 2000.
Moore, J. K., Abbott, M. R., Richman, J. G., Smith, W. O., Cowles, T. J., Coale, K. H., Gardner, W. D., and Barber, R. T.: SeaWiFS satellite ocean color data from the Southern Ocean, Geophys. Res. Lett., 26, 1465–1468, 1999.
Nishida, S.: Nannoplankton flora in the Southern Ocean, with special reference to siliceous varieties, Memoirs of National Institute of Polar Research, Special issue, 40, 56–68, 1986.
Odate, T. and Fukuchi, M.: Distribution and community structure of picophytoplankton in the Southern Ocean during the late austral summer of 1992, 86–100, 1995.
Orsi, A. H., Whitworth Iii, T., and Nowlin Jr, W. D.: On the meridional extent and fronts of the Antarctic Circumpolar Current, Deep-Sea Res. Pt. I, 42, 641–673, 1995.
Park, J., Oh, I.-S., Kim, H.-C., and Yoo, S.: Variability of SeaWiFs chlorophyll *a* in the southwest Atlantic sector of the Southern Ocean: Strong topographic effects and weak seasonality, Deep-Sea Res. Pt. I, 57, 604–620, 2010.
Parslow, J. S., Boyd, P. W., Rintoul, S. R., and Griffiths, F. B.: A persistent subsurface chlorophyll maximum in the Interpolar Frontal Zone south of Australia: Seasonal progression and implications for phytoplankton-light-nutrient interactions, J. Geophys. Res.-Oceans, 106, 31543–31557, 2001.
Passow, U.: Transparent exopolymer particles (TEP) in aquatic environments, Prog. Oceanogr., 55, 287–333, 2002.
Passow, U. and De La Rocha, C. L.: Accumulation of mineral ballast on organic aggregates, Global Biogeochem. Cy., 20, GB1013, doi:10.1029/2005GB002579, 2006.
Pilskaln, C. H., Manganini, S. J., Trull, T. W., Armand, L., Howard, W., Asper, V. L., and Massom, R.: Geochemical particle fluxes in the Southern Indian Ocean seasonal ice zone: Prydz Bay region, East Antarctica, Deep-Sea Res. Pt. I, 51, 307–332, 2004.
Pollard, R., Tréguer, P., and Read, J.: Quantifying nutrient supply to the Southern Ocean, J. Geophys. Res.-Oceans, 111, C05011, doi:10.1029/2005JC003076, 2006.
Pollard, R. T., Bathmann, U., Dubischar, C., Read, J. F., and Lucas, M.: Zooplankton distribution and behaviour in the Southern Ocean from surveys with a towed Optical Plankton Counter, Deep-Sea Res. Pt. II, 49, 3889–3915, 2002.

BGD
12, 8615–8690, 2015

Popp, B. N., Trull, T., Kenig, F., Wakeham, S. G., Rust, T. M., Tilbrook, B., Griffiths, B., Wright, S. W., Marchant, H. J., Bidigare, R. R., and Laws, E. A.: Controls on the carbon isotopic composition of southern ocean phytoplankton, Global Biogeochem. Cy., 13, 827–843, 1999.
Quéguiner, B.: Biogenic silica production in the Australian sector of the Subantarctic Zone of the Southern Ocean in late summer 1998, J. Geophys. Res.-Oceans, 106, 31627–31636, 2001.
Quéguiner, B.: Iron fertilization and the structure of planktonic communities in high nutrient regions of the Southern Ocean, Deep-Sea Res. Pt. II, 90, 43–54, 2013.
Raitsos, D. E., Lavender, S. J., Maravelias, C. D., Haralabous, J., Richardson, A. J., and Reid, P. C.: Identifying four phytoplankton functional types from space: An ecological approach, Limnol. Oceanogr., 53, 605–613, 2008.
Rembauville, M., Blain, S., Armand, L., Quéguiner, B., and Salter, I.: Export fluxes in a naturally iron-fertilized area of the Southern Ocean – Part 2: Importance of diatom resting spores and faecal pellets for export, Biogeosciences, 12, 3171–3195, doi:10.5194/bg-12-3171-2015, 2015.
Reynolds, R. W., Rayner, N. A., Smith, T. M., Stokes, D. C., and Wang, W.: An improved in situ and satellite SST analysis for climate, J. Climate, 15, 1609–1625, 2002.
Ridgway, K. R. and Dunn, J. R.: Observational evidence for a Southern Hemisphere oceanic supergyre, Geophys. Res. Lett., 34, L13612, doi:10.1029/2007GL030392, 2007.
Rigual-Hernández, A. S., Bárcena, M. A., Sierro, F. J., Flores, J. A., Hernández-Almeida, I., Sanchez-Vidal, A., Palanques, A., and Heussner, S.: Seasonal to interannual variability and geographic distribution of the silicoflagellate fluxes in the Western Mediterranean, Mar. Micropaleontol., 77, 46–57, 2010.
Rigual-Hernández, A. S., Sierro, F. J., Bárcena, M. A., Flores, J. A., and Heussner, S.: Seasonal and interannual changes of planktic foraminiferal fluxes in the Gulf of Lions (NW Mediterranean) and their implications for paleoceanographic studies: Two 12-year sediment trap records, Deep-Sea Res. Pt. I, 66, 26–40, 2012.
Rigual-Hernández, A. S., Bárcena, M. A., Jordan, R. W., Sierro, F. J., Flores, J. A., Meier, K. J. S., Beaufort, L., and Heussner, S.: Diatom fluxes in the NW Mediterranean: evidence from a 12-year sediment trap record and surficial sediments, J. Plankton Res., 35, 1109–1125, 2013.

BGD
12, 8615–8690, 2015

Rigual-Hernández, A. S., Trull, T. W., Bray, S. G., Closset, I., and Armand, L. K.: Seasonal dynamics in diatom and particulate export fluxes to the deep sea in the Australian sector of the southern Antarctic Zone, J. Mar. Sys., 142, 62–74, 2015.

Rintoul, S. R. and Bullister, J. L.: A late winter hydrographic section from Tasmania to Antarctica, Deep-Sea Res. Pt. I, 46, 1417–1454, 1999.

Rintoul, S. R. and Trull, T. W.: Seasonal evolution of the mixed layer in the Subantarctic zone south of Australia, J. Geophys. Res.-Oceans, 106, 31447–31462, 2001.

Romero, O. and Armand, L.: Marine diatoms as indicators of modern changes in oceanographic conditions, in: The Diatoms: Applications for the Environmental and Earth Sciences, edited by: Smol, J. P. and Stoermer, E. F., 373–400, 2010.

Romero, O., Lange, C. B., Fischer, G., Treppke, U. F., and Wefer, G.: Variability in export production documented by downward fl uxes and species composition of marine planktonic diatoms: observations from the tropical and equatorial Atlantic, in: The Use of Proxies in Paleoceanography – Examples from the South Atlantic, edited by: Fischer, G. and Wefer, G., Springer-Verlag Berlin Heidelberg, 365–392, 1999.

Romero, O. E., Fischer, G., Lange, C. B., and Wefer, G.: Siliceous phytoplankton of the western equatorial Atlantic: sediment traps and surface sediments, Deep-Sea Res. Pt. II, 47, 1939–1959, 2000.

Romero, O., Boeckel, B., Donner, B., Lavik, G., Fischer, G., and Wefer, G.: Seasonal productivity dynamics in the pelagic central Benguela System inferred from the flux of carbonate and silicate organisms, J. Mar. Sys., 37, 259–278, 2002.

Romero, O. E., Armand, L. K., Crosta, X., and Pichon, J. J.: The biogeography of major diatom taxa in Southern Ocean surface sediments: 3. Tropical/Subtropical species, Palaeogeogr. Palaeoecol., 223, 49–65, 2005.

Romero, O. E., Rixen, T., and Herunadi, B.: Effects of hydrographic and climatic forcing on diatom production and export in the tropical southeastern Indian Ocean, Mar. Ecol. Prog. Ser, 384, 69–82, 2009a.

Romero, O. E., Thunell, R. C., Astor, Y., and Varela, R. A.: Seasonal and interannual dynamics in diatom production in the Cariaco Basin, Venezuela, Deep-Sea Res. Pt. I, 56, 571–581, 2009b.

Romero, O. E., Kim, J. H., Bárcena, M. A., Hall, I. R., Zahn, R., and Schneider, R.: High-latitude forcing of diatom productivity in the southern Agulhas Plateau during the past 350 kyr, Paleoceanography, 30, 2014PA002636, doi:10.1002/2014PA002636, 2015.

BGD
12, 8615–8690, 2015

Rousseaux, C. S. and Gregg, W. W.: Climate variability and phytoplankton composition in the Pacific Ocean, J. Geophys. Res.-Oceans, 117, C10006, doi:10.1029/2012JC008083, 2012.
Sackett, O., Armand, L., Beardall, J., Hill, R., Doblin, M., Connelly, C., Howes, J., Stuart, B., Ralph, P., and Heraud, P.: Taxon-specific responses of Southern Ocean diatoms to Fe enrichment revealed by synchrotron radiation FTIR microspectroscopy, Biogeosciences, 11, 5795–5808, doi:10.5194/bg-11-5795-2014, 2014.
Sallée, J.-B., Wienders, N., Speer, K., and Morrow, R.: Formation of subantarctic mode water in the southeastern Indian Ocean, Ocean Dynam., 56, 525–542, 2006.
Salter, I., Kemp, A. E. S., Moore, C. M., Lampitt, R. S., Wolff, G. A., and Holtvoeth, J.: Diatom resting spore ecology drives enhanced carbon export from a naturally iron-fertilized bloom in the Southern Ocean, Global Biogeochem. Cy., 26, GB1014, doi:10.1029/2010GB003977, 2012.
Sancetta, C. and Calvert, S. E.: The annual cycle of sedimentation in Saanich inlet, British Columbia: implications for the interpretation of diatom fossil assemblages, Deep-Sea Res., 35, 71–90, 1988.
Sarmiento, J. L., Gruber, N., Brzezinski, M. A., and Dunne, J. P.: High-latitude controls of thermocline nutrients and low latitude biological productivity, Nature, 427, 56–60, 2004.
Scott, F. J. and Marchant, H. J.: Antarctic marine protists, 536 pp., 2005.
Sedwick, P. N., Edwards, P. R., Mackey, D. J., Griffiths, F. B., and Parslow, J. S.: Iron and manganese in surface waters of the Australian subantarctic region, Deep-Sea Res. Pt. I, 44, 1239–1253, 1997.
Sedwick, P. N., DiTullio, G. R., and Mackey, D. J.: Iron and manganese in the Ross Sea, Antarctica: Seasonal iron limitation in Antarctic shelf waters, J. Geophys. Res.-Oceans, 105, 11321–11336, 2000.
Sedwick, P. N., Bowie, A. R., and Trull, T. W.: Dissolved iron in the Australian sector of the Southern Ocean (CLIVAR SR3 section): Meridional and seasonal trends, Deep-Sea Res. Pt. I, 55, 911–925, 2008.
Selph, K. E., Landry, M. R., Allen, C. B., Calbet, A., Christensen, S., and Bidigare, R. R.: Microbial community composition and growth dynamics in the Antarctic Polar Front and seasonal ice zone during late spring 1997, Deep-Sea Res. Pt. II, 48, 4059–4080, 2001.
Shadwick, E. H., Trull, T. W., Tilbrook, B., Sutton, A. J., Schulz, E., and Sabine, C. L.: Seasonality of biological and physical controls on surface ocean CO2 from hourly observations

BGD
12, 8615–8690, 2015

at the Southern Ocean Time Series site south of Australia, Global Biogeochem. Cy., 29, GB004906, doi:10.1002/2014GB004906, 2015.
Shiono, M. and Koizumi, I.: Taxonomy of the *Thalassiosira trifulta* group in late neogene sediments from the northwest Pacific Ocean, Diatom Res., 15, 355–382, 2000.
Siegel, D. A. and Deuser, W. G.: Trajectories of sinking particles in the Sargasso Sea: modeling of statistical funnels above deep-ocean sediment traps, Deep-Sea Res. Pt. I, 44, 1519–1541, 1997.
Sigman, D. M., Hain, M. P., and Haug, G. H.: The polar ocean and glacial cycles in atmospheric CO_2 concentration, Nature, 466, 47–55, 2010.
Smetacek, V., Klaas, C., Menden-Deuer, S., and Rynearson, T. A.: Mesoscale distribution of dominant diatom species relative to the hydrographical field along the Antarctic Polar Front, Deep-Sea Res. Pt. II, 49, 3835–3848, 2002.
Smetacek, V., Assmy, P., and Henjes, J.: The role of grazing in structuring Southern Ocean pelagic ecosystems and biogeochemical cycles, Antarct. Sci., 16, 541–558, 2004.
Smetacek, V., Klaas, C., Strass, V. H., Assmy, P., Montresor, M., Cisewski, B., Savoye, N., Webb, A., d'Ovidio, F., Arrieta, J. M., Bathmann, U., Bellerby, R., Berg, G. M., Croot, P., Gonzalez, S., Henjes, J., Herndl, G. J., Hoffmann, L. J., Leach, H., Losch, M., Mills, M. M., Neill, C., Peeken, I., Rottgers, R., Sachs, O., Sauter, E., Schmidt, M. M., Schwarz, J., Terbruggen, A., and Wolf-Gladrow, D.: Deep carbon export from a Southern Ocean iron-fertilized diatom bloom, Nature, 487, 313–319, 2012.
Smith Jr., W. O., Keene, N. K., and Comiso, J. C.: Interannual Variability in Estimated Primary Productivity of the Antarctic Marginal Ice Zone, in: Antarctic Ocean and Resources Variability, edited by: Sahrhage, D., Springer Berlin Heidelberg, 131–139, 1988.
Smith Jr, W. O., Anderson, R. F., Keith Moore, J., Codispoti, L. A., and Morrison, J. M.: The US Southern Ocean Joint Global Ocean Flux Study: an introduction to AESOPS, Deep-Sea Res. Pt. II, 47, 3073–3093, 2000.
Sokolov, S. and Rintoul, S. R.: Circumpolar structure and distribution of the Antarctic Circumpolar Current fronts: 1. Mean circumpolar paths, J. Geophys. Res.-Oceans, 114, C11018, doi:10.1029/2008JC005108, 2009a.
Sokolov, S. and Rintoul, S. R.: Circumpolar structure and distribution of the Antarctic Circumpolar Current fronts: 2. Variability and relationship to sea surface height, J. Geophys. Res.-Oceans, 114, C11019, doi:10.1029/2008JC005248, 2009b.

BGD
12, 8615–8690, 2015

Sokolov, S. and Rintoul, S. R.: Structure of Southern Ocean fronts at 140° E, J. Mar. Sys., 37, 151–184, 2002.
Suzuki, H., Sasaki, H., and Fukuchi, M.: Short-term variability in the flux of rapidly sinking particles in the Antarctic marginal ice zone, Polar Biol., 24, 697–705, 2001.
Takahashi, K., Fujitani, N., and Yanada, M.: Long term monitoring of particle fluxes in the Bering Sea and the central subarctic Pacific Ocean, 1990–2000, Prog. Oceanogr., 55, 95–112, 2002.
Takeda, S.: Influence of iron availability on nutrient consumption ratio of diatoms in oceanic waters, Nature, 393, 774–777, 1998.
Taylor, S. R.: Abundance of chemical elements in the continental crust: a new table, Geochim. Cosmochim. Ac., 28, 1273–1285, 1964.
Taylor, S. R. and McLennan, S. M.: The Continental Crust: its Composition and Evolution, Boston, 312 pp., 1985.
Thomalla, S. J., Fauchereau, N., Swart, S., and Monteiro, P. M. S.: Regional scale characteristics of the seasonal cycle of chlorophyll in the Southern Ocean, Biogeosciences, 8, 2849–2866, doi:10.5194/bg-8-2849-2011, 2011.
Thunell, R., Pride, C., Ziveri, P., Muller-Karger, F., Sancetta, C., and Murray, D.: Plankton response to physical forcing in the Gulf of California, J. Plankton Res., 18, 2017–2026, 1996.
Tréguer, P. J.: The Southern Ocean silica cycle, Comptes Rendus Geoscience, 346, 279–286, 2014.
Tréguer, P. J. and De La Rocha, C. L.: The World Ocean Silica Cycle, Annu. Rev. Mar. Sci., 5, 477–501, 2013.
Tréguer, P., Nelson, D. M., Van Bennekom, A. J., Demaster, D. J., Quéguiner, B., and Leynaert, A.: The silica budget of the World Ocean: a re-estimate, Science, 268, 375–379, 1995.
Treppke, U. F., Lange, C. B., and Wefer, G.: Vertical fuxes of diatoms and silicofagellates in the eastern equatorial Atlantic, and their contribution to the sedimentary record, Mar. Micropaleontol., 28, 73–96, 1996.
Trull, T. W., Bray, S. G., Buesseler, K. O., Lamborg, C. H., Manganini, S., Moy, C., and Valdes, J.: In situ measurement of mesopelagic particle sinking rates and the control of carbon transfer to the ocean interior during the Vertical Flux in the Global Ocean (VERTIGO) voyages in the North Pacific, Deep-Sea Res. Pt. II, 55, 1684–1695, 2008.

BGD
12, 8615–8690, 2015

Trull, T. W., Bray, S. G., Manganini, S. J., Honjo, S., and François, R.: Moored sediment trap measurements of carbon export in the Subantarctic and Polar Frontal zones of the Southern Ocean, south of Australia, J. Geophys. Res.-Oceans, 106, 31489–31509, 2001a.

Trull, T. W., Sedwick, P. N., Griffiths, F. B., and Rintoul, S. R.: Introduction to special section: SAZ Project, J. Geophys. Res.-Oceans, 106, 31425–31429, 2001b.

Trull, T. W., Schulz, E., Bray, S. G., Pender, L., McLaughlan, D., Tilbrook, B., Rosenberg, M., and Lynch, T.: The Australian Integrated Marine Observing System Southern Ocean Time Series facility, 24–27 May 2010, 1–7, 2010.

Turner, J. T.: Zooplankton fecal pellets, marine snow an-d sinking phytoplankton blooms, Aquat. Microb. Ecol., 27, 57-102, 2002.

Venables, H. and Moore, C. M.: Phytoplankton and light limitation in the Southern Ocean: Learning from high-nutrient, high-chlorophyll areas, J. Geophys. Res.-Oceans, 115, C02015, doi:10.1029/2009JC005361, 2010.

Venrick, E. L., Lange, C. B., Reid, F. M. H., and Dever, E. P.: Temporal patterns of species composition of siliceous phytoplankton flux in the Santa Barbara Basin, J. Plankton Res., 30, 283–297, 2008.

Waite, A. M. and Nodder, S. D.: The effect of in situ iron addition on the sinking rates and export flux of Southern Ocean diatoms, Deep-Sea Res. Pt. II, 48, 2635–2654, 2001.

Wang, X., Matear, R. J., and Trull, T. W.: Modeling seasonal phosphate export and resupply in the Subantarctic and Polar Frontal zones in the Australian sector of the Southern Ocean, J. Geophys. Res.-Oceans, 106, 31525–31541, 2001.

Westwood, K. J., Brian Griffiths, F., Webb, J. P., and Wright, S. W.: Primary production in the Sub-Antarctic and Polar Frontal Zones south of Tasmania, Australia; SAZ-Sense survey, 2007, Deep-Sea Res. Pt. II, 58, 2162–2178, 2011.

Wright, S. W., Thomas, D. P., Marchant, H. J., Higgins, H. W., Mackey, M. D., and Mackey, D. J.: Analysis of phytoplankton of the Australian sector of the Southern Ocean: comparisons of microscopy and size frequency data with interpretations of pigment HPLC data using the \'CHEMTAX\' matrix factorisation program, Mar. Ecol.-Prog. Ser., 144, 285–298, 1996.

Yamanaka, Y. and Tajika, E.: The role of the vertical fluxes of particulate organic matter and calcite in the oceanic carbon cycle: Studies using an ocean biogeochemical general circulation model, Global Biogeochem. Cy., 10, 361–382, 1996.

BGD
12, 8615–8690, 2015

Yu, E. F., Francois, R., Bacon, M. P., Honjo, S., Fleer, A. P., Manganini, S. J., Rutgers van der Loeff, M. M., and Ittekot, V.: Trapping efficiency of bottom-tethered sediment traps estimated from the intercepted fluxes of 230Th and 231Pa, Deep-Sea Res. Pt. I, 48, 865–889, 2001.

Yuan, X.: High-wind-speed evaluation in the Southern Ocean, Journal of Geophysical Research: Atmospheres, 109, D13101, doi:10.1029/2003JD004179, 2004.

Zentara, S. J. and Kamykowski, D.: Geographic variations in the relationship between silicic acid and nitrate in the South Pacific Ocean, Deep-Sea Res., 28, 455–465, 1981.

Ziveri, P., Broerse, A. T. C., van Hinte, J. E., Westbroek, P., and Honjo, S.: The fate of coccoliths at 48° N 21° W, Northeastern Atlantic, Deep-Sea Res. Pt. II, 47, 1853–1875, 2000a.

Ziveri, P., Rutten, A., de Lange, G. J., Thomson, J., and Corselli, C.: Present-day coccolith fluxes recorded in central eastern Mediterranean sediment traps and surface sediments, Palaeogeogr. Palaeoecol., 158, 175–195, 2000b.

Ziveri, P., de Bernardi, B., Baumann, K.-H., Stoll, H. M., and Mortyn, P. G.: Sinking of coccolith carbonate and potential contribution to organic carbon ballasting in the deep ocean, Deep-Sea Res. Pt. II, 54, 659–675, 2007.

BGD
12, 8615–8690, 2015

Table 1. Deployment summary of sediment traps at stations 47, 54 and 61° S.

Site and trap designations	Hydrographic zone	Latitude ° S	Longitude ° E	Water column depth (m)	Trap depth (m)
47° S_1000	SAZ	46° 46° S	142° 4° E	4540	1060
54° S_800	PFZ	53° 45° S	141° 45° E	2280	830
61° S_2000	AZ	60° 44° S	139° 54° E	4393	2000

BGD
12, 8615–8690, 2015

Table 2. Individual cup fluxes for the < 1 mm fraction.

Deployment	Cup	Sampling period mid point	Length days	Diatoms 10^6 valves m^{-2} d^{-1}	Total Mass mg m^{-2} d^{-1}	$BSiO_2$ mg m^{-2} d^{-1}	%	$CaCO_3$ mg m^{-2} d^{-1}	%	POC mg m^{-2} d^{-1}	%
47° S 1000 m, 1999–2000	1	31/07/1999	20.0	0.002	19.6	0.8	4	8.6	44	3.0	15
	2	20/08/1999	20.0	0.113	27.1	3.4	13	15.3	57	2.8	10
	3	06/09/1999	15.0	0.195	45.9	5.1	11	26.2	57	4.2	9
	4	21/09/1999	15.0	0.147	57.5	5.4	9	36.0	63	4.4	8
	5	04/10/1999	10.0	0.213	66.5	7.9	12	46.8	70	4.2	6
	6	14/10/1999	10.0	0.364	65.9	3.8	6	46.1	70	4.2	6
	7	24/10/1999	10.0	0.137	89.8	4.3	5	66.4	74	5.3	6
	8	03/11/1999	10.0	0.080	73.9	3.8	5	56.9	77	4.1	6
	9	13/11/1999	10.0		12.7	0.2	2	9.1*	72*	1.1*	9*
	10	23/11/1999	10.0		4.2	0.2*	6*	3*	72*	0.5*	12*
	11	03/12/1999	10.0		4.3	0.2*	6*	3.1*	72*	0.5*	12*
	12	13/12/1999	10.0		13.8	0.8*	6*	9.9*	72*	2.0*	14*
	13	23/12/1999	10.0	0.049	32.6	2.4	7	19.3	59	3.7	11
	14	02/01/2000	10.0	0.001	38.5	2.2	6	25.0	65	3.6	9
	15	12/01/2000	10.0		15.9	0.1	1	9.5*	60*	1.9*	12*
	16	22/01/2000	10.0		14.0	0.6	5	8.4*	60*	1.6*	12*
	17	03/02/2000	15.0	0.002	11.4	0.2	2	6.8*	60*	1.1*	10*
	18	21/02/2000	20.0		8.0			4.8*	60*	1.0*	13*
	19	01/04/2000	60.0	0.110	39.6	2.9	7	23.4	59	4.7	12
	20	31/05/2000	60.0	0.125	47.0	5.1	11	33.2	71	3.3	7
	21	30/07/2000	60.0	0.002	13.0	0.7	5	7.4	57	1.6	12
47° S 1000 m, 2000–2001	1	13/10/2000	10.0		10.5	0.7	6	8.0	76	0.5	5
	2	23/10/2000	10.0		15.3	0.4	3	12.7	83	0.6	4
	3	02/11/2000	10.0	0.164	23.7	1.0	4	18.2	76	1.2	5
	4	12/11/2000	10.0	1.559	92.3	4.6	5	69.9	76	5.1	6
	5	22/11/2000	10.0	0.037	16.7	0.1	1	12.3*	74*	1.6*	10*
	6	02/12/2000	10.0	0.001	176.3						
	7	12/12/2000	10.0		9.9			5.7	57	1.5	15
	8	22/12/2000	10.0		8.9	0.1	1	5.2	59	0.8	9
	9	01/01/2001	10.0	0.053	30.4	1.6	5	20.5	67	2.3	8
	10	11/01/2001	10.0	0.345	51.3	3.2	6	35.2	69	3.6	7
	11	21/01/2001	10.0	0.200	48.4	5.1	10	32.8	68	3.2	7
	12	31/01/2001	10.0	0.089	21.1	1.4	6	13.5	64	2.0	9
	13	10/02/2001	10.0	0.077	62.0	3.3	5	47.5	77	3.3	5
	14	20/02/2001	10.0	0.435	75.4	4.1	5	58.8	78	3.6	5
	15	02/03/2001	10.0	0.758	89.4	6.5	7	69.1	77	4.2	5
	16	14/03/2001	15.0	0.398	104.8	9.1	9	87.3	83	3.5	3
	17	29/03/2001	15.0		64.0*	5.3*	8*	50.0*	78*	2.9*	5*
	18	03/05/2001	55.0	0.231	52.9	4.2	8	39.9	75	2.7	5
	19	30/06/2001	60.0	0.293	32.2	1.8	6	23.9	74	1.9	6
	20	29/08/2001	60.0	0.126	19.8	1.4	7	15.7	79	1.3	6
	21	13/10/2001	30.0	0.038	9.7	0.4	5	5.4	56	1.4	14

BGD
12, 8615–8690, 2015

Table 2. Continued.

Deployment	Cup	Sampling period mid point	Length days	Diatoms 10^6 valves m^{-2} d^{-1}	Total Mass mg m^{-2} d^{-1}	$BSiO_2$ mg m^{-2} d^{-1}	%	$CaCO_3$ mg m^{-2} d^{-1}	%	POC mg m^{-2} d^{-1}	%
54° S 800 m, 1997–1998	1	26/09/1997	8.5	0.275	2.7	1.4*	53*	0.7	27	0.1*	3*
	2	04/10/1997	8.5		11.5	6.1*	53*	3.1	27	0.3*	3*
	3	13/10/1997	8.5		11.5	6.1*	53*	3.1	27	0.3*	3*
	4	21/10/1997	8.5	4.561	47.0	25.1	53	12.6	27	1.4	3
	5	30/10/1997	8.5	13.121	100.0	52.5	53	26.0	26	2.7	3
	6	07/11/1997	8.5	20.564	141.7	79.3	56	35.5	25	2.3	2
	7	16/11/1997	8.5	26.211	233.5	131.7	56	56.4	24	4.3	2
	8	24/11/1997	8.5	11.542	165.8	81.7	49	45.8	28	4.4	3
	9	03/12/1997	8.5	4.914	53.3	13.1	25	20.5	38	2.4	4
	10	11/12/1997	8.5		63.2	20.5	33	16.6	26	2.5	4
	11	20/12/1997	8.5	11.711	148.2	63.8	43	26.5	18	5.0	3
	12	28/12/1997	8.5	20.881	111.9	38.8	35	29.7	27	4.6	4
	13	04/01/1998	4.3	34.729	109.7	51.2	47	29.5	27	4.9	5
	14	08/01/1998	4.3		99.9	54.2	54	23.0	23	4.5	5
	15	12/01/1998	4.3		151.8	92.7	61	28.7	19	4.0	3
	16	16/01/1998	4.3		153.0	87.8	57	31.5	21	5.8	4
	17	21/01/1998	4.3	70.808	265.5	164.7	62	50.6	19	8.8	3
	18	25/01/1998	4.3	54.059	396.0	259.2	65	66.0	17	9.9	2
	19	31/01/1998	8.5	41.101	276.2	171.7	62	47.2	17	7.0	3
	20	09/02/1998	8.5	28.947	141.7	74.3	52	37.0	26	4.6	3
	21	17/02/1998	8.5		66.4	30.5	46	20.4	31	2.3	3
54° S 800 m, 1999–2000	1	31/07/1999	20.0	9.681	45.9	34.3	75	1.8	4	1.3	3
	2	20/08/1999	20.0	10.944	71.8	52.8	74	3.2	4	0.9	1
	3	06/09/1999	15.0	7.948	81.4	63.2	78	3.6	4	1.1	1
	4	21/09/1999	15.0	4.867	25.1	17.1	68	2.6	10	0.9	3
	5	04/10/1999	10.0	5.622	44.5	31.9	72	3.2	7	1.0	2
	6	14/10/1999	10.0	9.942	101.1	70.8	70	5.8	6	1.1	1
	7	24/10/1999	10.0	8.689	58.2	37.6	65	6.2	11	1.1	2
	8	03/11/1999	10.0	5.857	106.3	62.0	58	11.3	11	3.9	4
	9	13/11/1999	10.0	6.081	121.9	80.3	66	20.2	17	2.6	2
	10	23/11/1999	10.0	28.312	294.4	170.7	58	63.8	22	7.1	2
	11	03/12/1999	10.0	51.610	514.8	302.5	59	108.5	21	16.7	3
	12	13/12/1999	10.0	10.590	724.4	429.3	59	142.5	20	23.0	3
	13	23/12/1999	10.0	15.287	660.6	396.3	60	106.2	16	20.0	3
	14	02/01/2000	10.0	19.142	511.0	309.1	61	57.8	11	16.4	3
	15	12/01/2000	10.0	17.274	338.7	207.0	61	35.5	10	9.5	3
	16	22/01/2000	10.0		11.3	6.3	56	2.3	20	0.4	3
	17	03/02/2000	15.0	3.892	104.4	35.7	34	52.3	50	3.4	3
	18	21/02/2000	20.0	11.224	193.9	118.8	61	34.4	18	4.1	2
	19	01/04/2000	60.0	4.764	132.0	69.4	53	28.7	22	2.8	2
	20	31/05/2000	60.0	3.390	50.1	31.5	63	5.8	12	1.4	3
	21	30/07/2000	60.0	1.117	36.9	20.3	55	4.7	13	1.3	3

BGD
12, 8615–8690, 2015

Table 2. Continued.

Deployment	Cup	Sampling period mid point	Length days	Diatoms 10^6 valves m^{-2} d^{-1}	Total Mass mg m^{-2} d^{-1}	$BSiO_2$ mg m^{-2} d^{-1}	%	$CaCO_3$ mg m^{-2} d^{-1}	%	POC mg m^{-2} d^{-1}	%
54° S 800 m, 2002–2003	1	23/11/2002	10.0	5.789	96.7	46.8	48	18.3	19	3.6	4
	2	03/12/2002	10.0	27.759	190.6	110.6	58	37.5	20	4.6	2
	3	13/12/2002	10.0	65.376	363.9	203.6	56	81.0	22	12.3	3
	4	23/12/2002	10.0	36.000	240.7	134.0	56	47.2	20	11.4	5
	5	02/01/2003	10.0	6.766	125.6	54.4	43	45.4	36	4.8	4
	6	12/01/2003	10.0	18.438	158.9	93.7	59	35.0	22	5.4	3
	7	22/01/2003	10.0	28.832	360.2	219.1	61	68.9	19	8.6	2
	8	01/02/2003	10.0	45.008	213.8	113.7	53	48.3	23	5.5	3
	9	11/02/2003	10.0	28.106	396.5	253.8	64	56.0	14	5.1	1
	10	21/02/2003	10.0	16.957	60.8	26.6	44	23.7	39	2.2	4
	11	03/03/2003	10.0	1.902	58.5	16.8	29	23.8	41	5.5	9
	12	13/03/2003	10.0	1.462	89.3	26.6	30	37.0	41	7.0	8
	13	23/03/2003	10.0	2.326	49.5	13.6	28	25.1	51	3.4	7
	14	02/04/2003	10.0	0.995	33.5	7.6	23	18.2	54	2.7	8
	15	12/04/2003	10.0	1.192	31.9	6.2	19	20.1	63	1.6	5
	16	22/04/2003	10.0	0.724	21.6	5.8*	27*	14.0	65	1.0	4
	17	09/05/2003	25.0	1.996	23.8	7.3	31	12.8	54	0.9	4
	18	11/06/2003	40.0	1.625	23.7	10.8	46	7.8	33	1.0	4
	19	23/07/2003	45.0	1.226	16.9	8.0	47	5.5	33	0.7	4
	20	25/08/2003	20.0	2.606	33.6	13.5	40	11.9	35	1.8	5
	21	15/09/2003	23.0		33.6						
54° S 800 m, 2003–2004	1	04/10/2003	14.0	0.352	15.1	8.1*	54*	4.5*	30*	0.5*	3*
	2	18/10/2003	14.0	1.143	23.4	12.6	54	7.0	30	0.8	3
	3	01/11/2003	14.0	2.808	34.8	18.6	54	10.8	31	1.1	3
	4	15/11/2003	14.0	11.519	121.0	54.6	45	19.9	16	2.0	2
	5	29/11/2003	14.0	7.748	75.5	35.9	48	14.6	19	1.6	2
	6	13/12/2003	14.0	19.892	178.6	111.6	62	40.2	23	3.6	2
	7	27/12/2003	14.0	10.320	232.6	134.8	58	43.6	19	7.2	3
	8	10/01/2004	14.0	30.998	182.0	114.5	63	33.7	19	6.2	3
	9	24/01/2004	14.0	16.786	121.9	81.7	67	21.0	17	3.3	3
	10	07/02/2004	14.0	11.142	63.9	37.0	58	10.8	17	2.7	4
	11	21/02/2004	14.0	5.982	28.5	16.6	58	7.0	24	1.0	4
	12	06/03/2004	14.0	6.189	31.0	18.4	59	7.7	25	0.9	3
	13	20/03/2004	14.0	9.824	66.2	45.3	68	10.2	15	1.0	2
	14	03/04/2004	14.0	11.515	84.6	52.6	62	16.9	20	0.8	1
	15	17/04/2004	14.0	0.622	15.6	10.1*	65*	4.9	31	0.8	5
	16	01/05/2004	14.0	0.658	10.6	6.9*	65*	4.0	38	0.5	4
	17	25/05/2004	35.0	3.431	19.6	13.7	70	3.5	18	0.4	2
	18	29/06/2004	35.0	1.549	19.3	11.3	59	4.5	23	1.1	6
	19	03/08/2004	35.0	1.235	14.5	6.0	41	2.8	20	2.0	14
	20	07/09/2004	35.0	1.088	10.3	5.0	49	3.8	37	0.5	5
	21	02/10/2004	14.0	0.458	7.3	3.6	49	2.5	34	0.5	7

BGD
12, 8615–8690, 2015

Table 2. Continued.

Deployment	Cup	Sampling period mid point	Length days	Diatoms 10^6 valves m^{-2} d^{-1}	Total Mass mg m^{-2} d^{-1}	$BSiO_2$ mg m^{-2} d^{-1}	%	$CaCO_3$ mg m^{-2} d^{-1}	%	POC mg m^{-2} d^{-1}	%
54° S 800 m, 2005–2006	1	22/12/2005	17.0	24.184	197.9	120.0	61	43.5	22	4.6	2
	2	08/01/2006	17.0	19.228	193.6	115.2	59	47.5	25	3.2	2
	3	25/01/2006	17.0	47.595	418.1	275.3	66	65.1	16	12.2	3
	4	11/02/2006	17.0	11.571	178.0	60.8	34	92.1	52	3.9	2
	5	28/02/2006	17.0	4.840	116.7	31.7	27	66.9	57	2.4	2
	6	17/03/2006	17.0	1.180	44.9	7.9	17	30.1	67	1.5	3
	7	03/04/2006	17.0	8.853	110.6	46.0	42	50.2	45	2.6	2
	8	20/04/2006	17.0	11.216	142.8	86.5	61	33.0	23	3.1	2
	9	07/05/2006	17.0	9.477	107.0	63.5	59	23.3	22	2.6	2
	10	07/06/2006	45.0	0.904	18.6	7.6	41	8.0	43	0.6	3
	11	22/07/2006	45.0	0.072	3.6	1.6*	45*	1.2	33	0.4	10
	12	05/09/2006	45.0	0.778	9.1	4.6	50	2.8	31	0.3	3
	1	18/10/2006	16.0	0.291	6.4	1.9*	29*	1.0	15	0.4	7
	2	03/11/2006	16.0	1.065	23.9	6.9	29	3.4	14	1.2	5
	3	19/11/2006	16.0	4.461	77.6	25.1	32	13.6	18	3.4	4
	4	05/12/2006	16.0	23.929	131.5	71.5	54	28.7	22	4.5	3
	5	21/12/2006	16.0	72.099	333.9	220.9	66	30.8	9	10.5	3
	6	06/01/2007	16.0	100.622	335.5	243.5	73	18.4	5	9.5	3
	7	22/01/2007	16.0	0.014	0.8	0.6*	72*	0.1	7	0.0*	3*
	8	07/02/2007	16.0	0.028	1.0	0.7*	72*	0.1*	11*	0.0*	2*
	9	23/02/2007	16.0	0.012	0.6	0.4*	72*	0.1*	11*	0.0*	2*
	10	11/03/2007	16.0	0.021	0.6	0.4*	72*	0.1*	11*	0.0*	2*
	11	27/03/2007	16.0	7.500	33.0	22.8	69	3.8	12	1.1	3
	12	12/04/2007	16.0	0.030	1.8	1.2*	69*	0.8	43	0.1	4
	13	28/04/2007	16.0	0.106	6.2	4.3*	69*	4.1	67	0.1	2
	14	14/05/2007	16.0	0.010	0.7	0.5*	69*	0.3*	51	0.0*	3*
	15	30/05/2007	16.0	0.013	0.5	0.4*	69*	0.3*	51*	0.0*	3*
	16	18/06/2007	23.0	0.420	9.0	6.2*	69*	3.9	43	0.3	3
	17	11/07/2007	23.0	0.005	0.3	0.2*	69*	0.2*	43*	0.0*	3*
	18	03/08/2007	23.0	0.001	0.2	0.2*	69*	0.1*	43*	0.0*	3*
	19	23/08/2007	16.0	0.001	0.1	0.1*	69*	0.0*	43*	0.0*	3*
	20	08/09/2007	16.0	0.140	4.2	2.9*	69*	1.9	45	0.1	3
	21	24/09/2007	16.0	0.067	3.1	2.2*	69*	1.3	42	0.2	6

* Component fluxes representing intervals for which insufficient material was available for component measurement and were estimated.

BGD
12, 8615–8690, 2015

Table 3. Estimated annual export fluxes of total mass flux, biogenic silica, calcium carbonate, POC and diatom valves for < 1 mm fraction at the 47, 54 and 61° S sites.

(a) Annual fluxes of biogeochemical components ($g\,m^{-2}\,yr^{-1}$) and diatom valves (valves $10^8\,m^{-2}\,yr^{-1}$)

Trap	Year	Total mass flux	SiO_2-bio	PIC as $CaCO_3$	POC	Diatom valves ($\times 10^8$)
47_1000	1999–2000	12	1	8	1.1	0.3
	2000–2001	15	1	12	0.9	0.8
	Average ± SD	14 ± 2	1 ± 0	10 ± 3	1.0 ± 0.1	0.5 ± 0.4
54_800	1997–1998	19	10	4	0.6	30.2
	1999–2000	52	31	9	1.4	29.1
	2002–2003	30	16	8	1.1	39.0
	2003–2004	20	12	4	0.6	22.5
	2005–2006	29	15	9	0.7	30.8
	2006–2007	16	10	2	0.5	34.5
	Average ± SD	24 ± 13	12 ± 9	7 ± 3	0.8 ± 0.4	31.0 ± 5.5
61_2000	2001–2002	85	65	6	1.2	242.9

BGD
12, 8615–8690, 2015

Table 3. Continued.

(b) Proportion of biogeochemical components (wt %)				
Trap	Year	SiO_2-bio	PIC as $CaCO_3$	POC
47_1000	1999–2000	8	65	9.0
	2000–2001	7	76	5.6
	Average ± SD	7 ± 1	70 ± 8	7.3 ± 2.4
54_800	1997–1998	53	23	2.9
	1999–2000	60	17	2.7
	2002–2003	52	25	3.5
	2003–2004	59	20	3.1
	2005–2006	53	30	2.5
	2006–2007	63	12	3.3
	Average ± SD	57 ± 4	21 ± 7	3.0 ± 0.4
61_2000	2001–2002	76	7	1.4

BGD
12, 8615–8690, 2015

Table 3. Continued.

(c) Annual fluxes of biogeochemical elements, mmol m^{-2} yr^{-1} and mole ratios						
Trap	Year	BSi	PIC	POC	BSi : PIC	POC : BSi
47_1000	1999–2000	15	76	89	0.2	5.7
	2000–2001	17	116	72	0.1	4.2
	Average ± SD	16 ± 1	96 ± 28	80 ± 12	0.2 ± 0.0	4.9 ± 1.1
54_800	1997–1998	168	43	46	3.9	0.3
	1999–2000	513	87	117	5.9	0.2
	2002–2003	264	77	89	5.9	0.3
	2003–2004	192	40	50	4.8	0.3
	2005–2006	252	87	59	2.9	0.2
	2006–2007	168	19	43	8.9	0.3
	Average ± SD	259 ± 131	59 ± 29	67 ± 29	5.4 ± 2.1	0.3 ± 0.0
61_2000	2001–2002	1081	63	102	17.3	0.1

BGD
12, 8615–8690, 2015

Table 4. List of diatom species recorded in the sediment traps of the 47, 54 and 61° S (2000 m) sites along the 140° E. Relative abundances < 0.1 are represented by an asterisk (*), whereas the absence of a taxon in a given site is represented by an empty circle (○).

Species	SAZ (47° S)	PFZ (54° S)	AZ (61° S)
Actinocyclus actinochilus (Ehrenberg) Simonsen	*	○	*
Actinocyclus curvatulus Janisch	0.3	*	○
Actinocyclus exiguus Fryxell et Semina	*	○	○
*Actinocyclus octonarius*Ehrenberg	*	○	○
Actinocyclus spp.	0.6	*	*
Alveus marinus (Grunow) Kaczmarska et Fryxell	*	○	○
Asteromphalus hookeri Ehrenberg	*	0.5	0.2
A. hyalinus Karsten	*	0.2	0.2
A. parvulus Karsten	*	0.1	0.2
Asteromphalus spp.	○	○	*
Azpeitia tabularis (Grunow) Fryxell et Sims	10.8	0.8	0.7
Chaetoceros aequatorialis var. *antarcticus* Manguin	○	0.1	*
Ch. atlanticus Cleve	0.1	0.5	0.2
Ch. dichaeta Ehrenberg	○	0.6	0.1
Ch. peruvianus Brightwell	0.1	*	○
Chaetoceros subgenus *Hyalochaete* spp.	0.2	0.4	0.2
Chaetoceros subgenus *Phaeoceros* spp.	○	0.1	0.2
Chaetoceros resting spores	2.3	0.5	0.1
Cocconeis spp.	0.2	○	○
Corethron sp.	*	*	*
Cyclotella spp.	*	○	○
Dactyliosolen antarcticus Castracane			
Diploneis bombus (Ehrenberg) Ehrenberg	*	○	○
Eucampia antarctica (Castracane) Mangin (summer form)	○	0.3	○
E. antarctica (Castracane) Mangin (winter form)	*	*	0.1
Fragilariopsis curta (Van Heurck) Hustedt	○	*	0.6
F. cylindrus (Grunow) Krieger	○	*	0.2
F. doliolus (Wallich) Medlin et Sims	0.5	○	○
F. kerguelensis (O'Meara) Hustedt	43	59.3	79.9
F. obliquecostata (van Heurck) Heiden	○	*	*
F. pseudonana (Hasle) Hasle	*	3.1	2
F. rhombica (O'Meara) Hustedt	0.4	2.3	0.9
F. ritscherii Hustedt	0.4	0.1	0.1
F. separanda Hustedt	○	0.1	2.1
F. cf. *sublineata* (Van Heurck) Heiden	○	○	*
Fragilariopsis spp.	○	*	○

BGD
12, 8615–8690, 2015

Table 4. Continued.

Species	SAZ (47° S)	PFZ (54° S)	AZ (61° S)
Gyrosigma spp.	○	*	○
Haslea trompii (Cleve) Simonsen	○	0.1	*
Hemidiscus cuneiformis Wallich	3.7	○	○
Navicula directa (Smith) Ralfs in Pritchard	○	4.6	0.3
Nitzschia bicapitata Cleve	2.8	*	○
N. braarudii (Hasle)	0.2	○	○
N. kolaczeckii Grunow	0.6	*	○
N. sicula (Castracane) Hustedt var. *bicuneata* Grunow	2	*	0.1
N. sicula (Castracane) Hustedt var. *rostrata* Hustedt	*	*	○
Nitzschia spp.	*	*	○
Paralia spp.	*	○	○
Pleurosigma spp.	0.2	0.1	*
Porosira pseudodenticulata (Hustedt) Jousé	0.1	*	*
Proboscia alata (Brightwell) Sundström	0.1	*	○
P. inermis (Castracane) Jordan Ligowski	○	*	○
Proboscia spp.	*	*	○
Psammodiction panduriforme (Gregory) Mann	0.1	○	○
Pseudo-nitzschia cf. *lineola*	*	8.1	0.4
P-n. heimii Manguin	*	4.6	*
Pseudo-nitzschia spp.	*	○	0.1
Rhizosolenia antennata (Ehrenberg) Brown f. *antennata*	*	*	○
R. antennata (Ehrenberg) Brown f. *semispina* Sundström	0.1	*	○
R. bergonii Peragallo	1.8	*	○
Rhizosolenia cf. *costata*	○	*	○
R. curvata Zacharias	○	*	○
R. polydactyla Castracane f. *polydactyla*	*	*	○
Rhizosolenia sp. f. 1A (Armand et Zielinski)	○	*	*
Rhizosolenia spp.	0.2	*	0.1
Roperia tesselata (Roper) Grunow	3.2	*	○
Stellarima stellaris (Roper) Hasle et Sims	0.5	*	○
Thalassionema nitzschioides var. *capitulata* (Castracane) Moreno-Ruiz	*	0.2	0.1
T. nitzschioides var. *lanceolata* (Grunow) Pergallo et Pergallo	0.2	0.9	0.1
T. nitzschioides var. *parvum*Moreno-Ruiz	*	*	○
T. nitzschioides var. 1 (Zielinski et Gersonde)	0.2	0.4	○
Thalassiosira eccentrica (Ehrenberg) Cleve	0.9	0.1	0.2

BGD
12, 8615–8690, 2015

Table 4. Continued.

Species	SAZ (47° S)	PFZ (54° S)	AZ (61° S)
T. ferelineata Hasle et.Fryxell	0.3	○	○
T. gracilis var. *expecta* (Van Landingham) Frxyell et Hasle	0.1	0.7	0.4
T. gracilis var. *gracilis* (Karsten) Hustedt	0.3	3.9	3.6
T. gracilis group	0.3	4.6	4.1
T. gravida Cleve	○	○	*
T. lentiginosa (Janisch) Fryxell	2.1	2.1	5
T. leptopus (Grunow ex Van Heurck) Hasle et G.Fryxell	○	○	*
T. lineata Jousé	2.2	○	○
T. maculata Fryxell et Johans.	0.2	0.1	*
T. oestrupii (Ostenfeld) Hasle var. *oestrupii* Fryxell et. Hasle	3.6	0.3	*
T. oestrupii (Ostenfeld) Hasle var. *venrickae* Fryxell et. Hasle	0.6	0.1	○
T. oliveriana(O'Meara) Makarova et Nikolaev	0.1	0.6	0.7
T. symmetrica Fryxell et Hasle	0.3	*	○
T. trifulta Fryxell	0.1	○	○
T. tumida (Janisch) Hasle	0.2	0.3	0.1
Thalassiosira sp. 1	5.4	0.1	*
Thalassiosira sp. 2	0.2	0.1	○
Thalassiosira sp. 3	○	0.2	○
Thalassiosira eccentric group	0.1	○	○
T. linear group	0.2	*	0.1
T. trifulta group	1.9	0.1	○
Thalassiosira spp. 20 µm	0.9	1.4	0.4
Thalassiosira spp. > 20 µm	1.7	0.1	*
Thalassiothrix antarctica Schimper ex Karsten	2.2	0.4	0.2
Trachyneis aspera (Ehrenberg) Cleve	○	○	○
Trichotoxon reinboldii (Van Heurck) Reid et Round	○	*	○
Tropidoneis group	*	0.4	*
Other centrics	1.2	0.1	*
Other pennates	0.2	*	0.1
Shannon's diversity index	2.48	1.86	1.04

BGD
12, 8615–8690, 2015

Table 5. Varimax loadings matrix (rotation: varimax normalized). Factor loadings for analysis on sediment trap samples using species and group of species with abundances higher than 1 % of the total integrated diatom assemblage for the whole sampling period at the 47° S (a) and 54° S site (b). Bold print indicates the dominant species or group of species within each factor (loadings > 0.70).

(a) 47° S site				
	Factor 1	Factor 2	Factor 3	Factor 4
Fragilariopsis kerguelensis	0.05	**−0.73**	−0.46	−0.35
Azpeitia tabularis	0.59	0.38	0.06	0.55
Thalassiosira sp. 1	−0.11	**0.91**	−0.17	−0.21
Nitzschia bicapitata	**−0.82**	0.41	0.09	0.19
Chaetoceros resting spores	−0.59	0.12	0.56	0.08
Thalassiosira oestrupii var. oestrupii	−0.06	**−0.75**	0.20	0.13
Hemidiscus cuneiformis	0.63	0.47	0.03	−0.09
Roperia tesselata	0.04	−0.29	**0.73**	0.11
Thalassiothrix antarctica	0.06	−0.05	0.05	0.61
Nitzschia sicula var. bicuneata	−0.64	−0.09	−0.03	−0.08
Thalassiosira lineata	0.15	0.02	**0.78**	−0.39
Rhizosolenia bergonii	0.08	0.14	0.17	−0.57
Thalassiosira lentiginosa	0.47	−0.16	0.15	0.29
Thalassiosira trifulta group	−0.53	−0.04	−0.06	−0.57
Variance (%)	19	19	13	13
Cumulative variance	19	38	51	64

(b) 54° S site			
Diatom species or groups of species	Factor 1	Factor 2	Factor 3
Fragilariopsis kerguelensis	**−0.91**	−0.20	−0.11
Navicula directa	**0.84**	−0.14	0.17
Pseudo-nitzschia heimii	0.35	**0.70**	0.36
Pseudo-nitzschia cf. *lineola*	**0.77**	0.25	0.41
Thalassiosira gracilis group	**0.81**	−0.19	0.19
Fragilariopsis pseudonana	**0.79**	0.09	−0.08
Fragilariopsis rhombica	**0.85**	0.29	0.14
Thalassiosira lentiginosa	0.09	**−0.89**	0.00
Chaetoceros group	0.12	0.12	**0.93**
Variance (%)	48	17	14
Cumulative total variance (%)	48	65	79

Note: Bold values highlight the taxa that define each factor.

BGD
12, 8615–8690, 2015

Table 6. Correlation coefficients between the PCA factors and the fluxes of bulk components (total mass, carbonate, biogenic silica and POC) for the 47° S (a) and 54° S (b) sites.

(a) 47 S site				
	Factor 1	Factor 2	Factor 3	Factor 4
Total mass	−0.10	−0.14	0.01	−0.19
Biogenic Silica	−0.09	−0.10	0.12	−0.11
Carbonate	−0.07	−0.18	−0.03	−0.20
POC	−0.28	0.06	0.14	−0.12
(b) 54 S site				
	Factor 1	Factor 2	Factor 3	
Total mass	**0.73**	0.07	0.03	
Biogenic Silica	**0.71**	0.08	−0.01	
Carbonate	0.66	0.06	0.15	
POC	**0.75**	0.12	0.06	

Note: Bold values are significant at $p < 0.05$.

BGD
12, 8615–8690, 2015

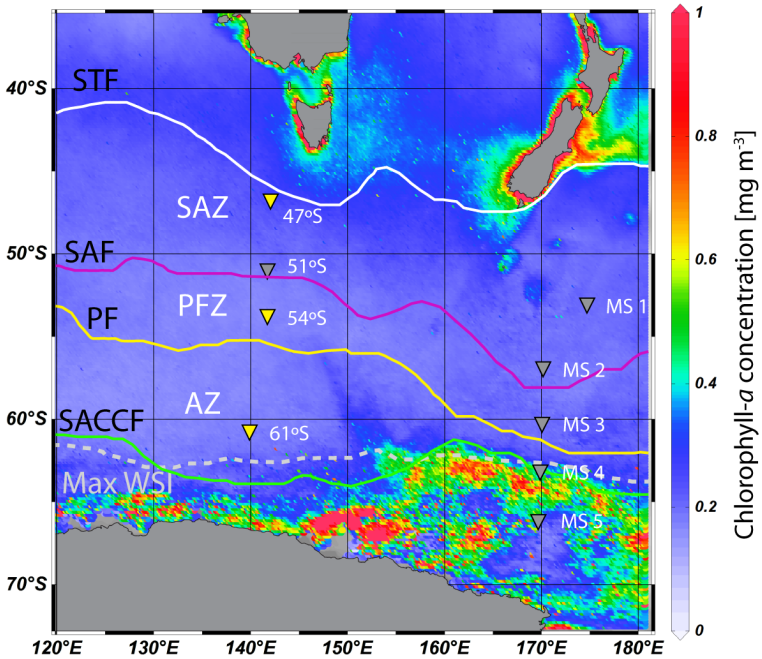

Figure 1. Southern Ocean chlorophyll *a* composite map (September 1997 to September 2007) from Seaviewing Wide Field-of-view Sensor with the location of the sediment trap moorings of the SAZ (47, 51, 54 and 61° S) and AESOPS (MS-1, MS-2, MS-3, MS-4 and MS-5) experiments. Abbreviations: STF Subtropical Front, SAZ Subantarctic Zone, SAF Subantarctic Front, PFZ Polar Frontal Zone, PF Polar Front, AZ Antarctic Zone SACC Southern extent of the Antarctic Circumpolar Current, Max WSI maximum winter sea ice extent. Oceanic fronts from Orsi et al. (1995). Sea ice extent from Fetterer et al. (2002, updated 2009).

BGD
12, 8615–8690, 2015

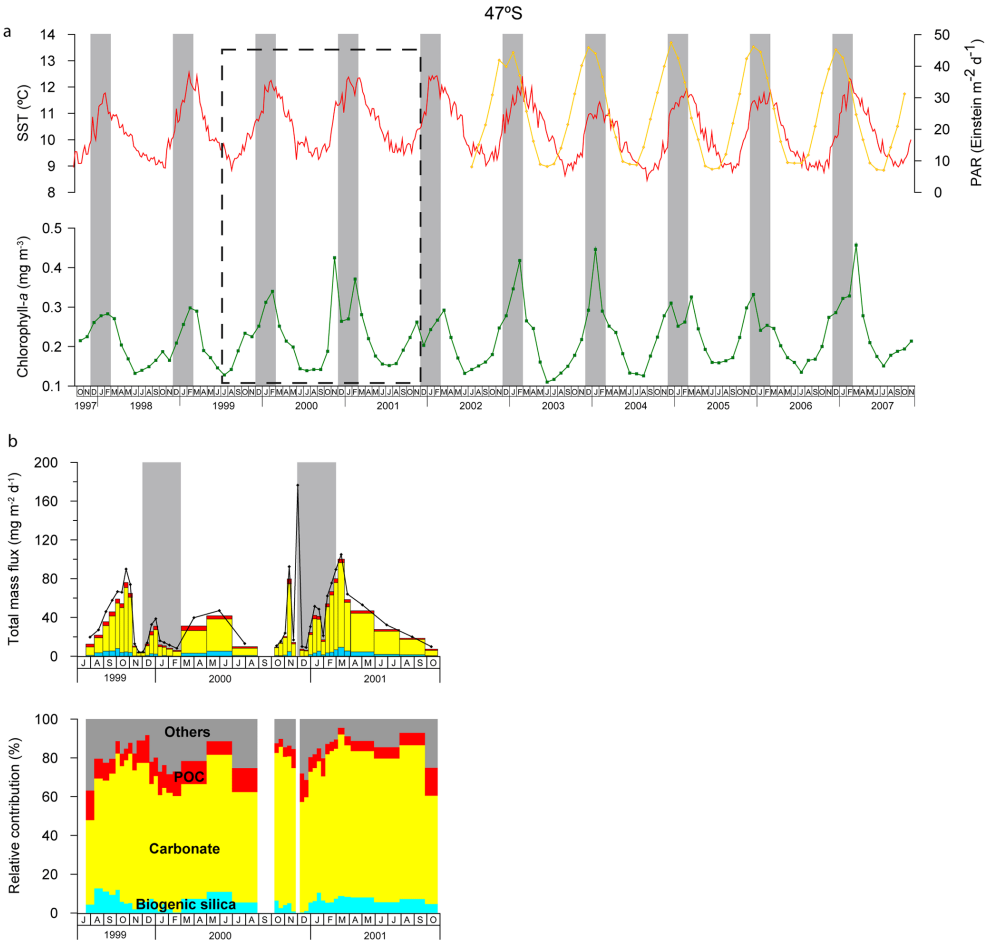

BGD
12, 8615–8690, 2015

Latitudinal and temporal distributions of diatom populations

A. S. Rigual-Hernández et al.

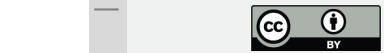

Figure 2. (a) Available mean sea surface temperature (SST), Photosynthetically Available Radiation (PAR), and Chlorophyll *a* concentration for the 47° S site. The dashed intervals represent the studied periods. **(b)** Temporal variability of the total mass and major component fluxes and of the relative contribution of biogenic silica, carbonate, particulate organic carbon (POC), and others for the < 1 mm fraction at 1000 m water depth at the 47° S site for the period July 1999–October 2001. Gray horizontal bars highlight the summer period (December to February) of each year.

BGD
12, 8615–8690, 2015

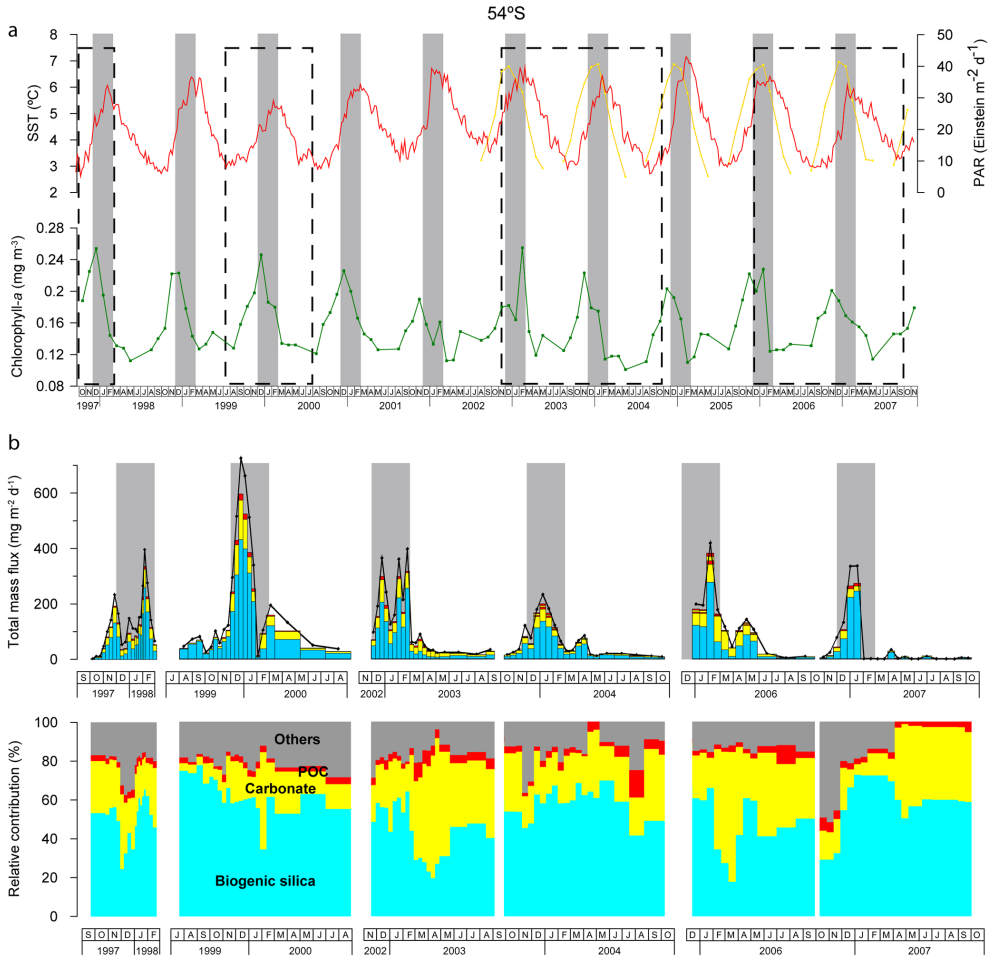

BGD
12, 8615–8690, 2015

Latitudinal and temporal distributions of diatom populations

A. S. Rigual-Hernández et al.

CC BY

Figure 3. (a) Available mean sea surface temperature (SST), Photosynthetically Available Radiation (PAR), and Chlorophyll *a* concentration for the 54° S site. The dashed intervals represent the studied periods. **(b)** Temporal variability of the total mass and major component fluxes and of the relative contribution of biogenic silica, carbonate, particulate organic carbon (POC), and others for the < 1 mm fraction at 800 m water depth at the 54° S site for the periods July 1999–August 2000, November 2002–October 2004 and December 2005–October 2007. Gray horizontal bars highlight the summer period (December to February) of each year.

BGD
12, 8615–8690, 2015

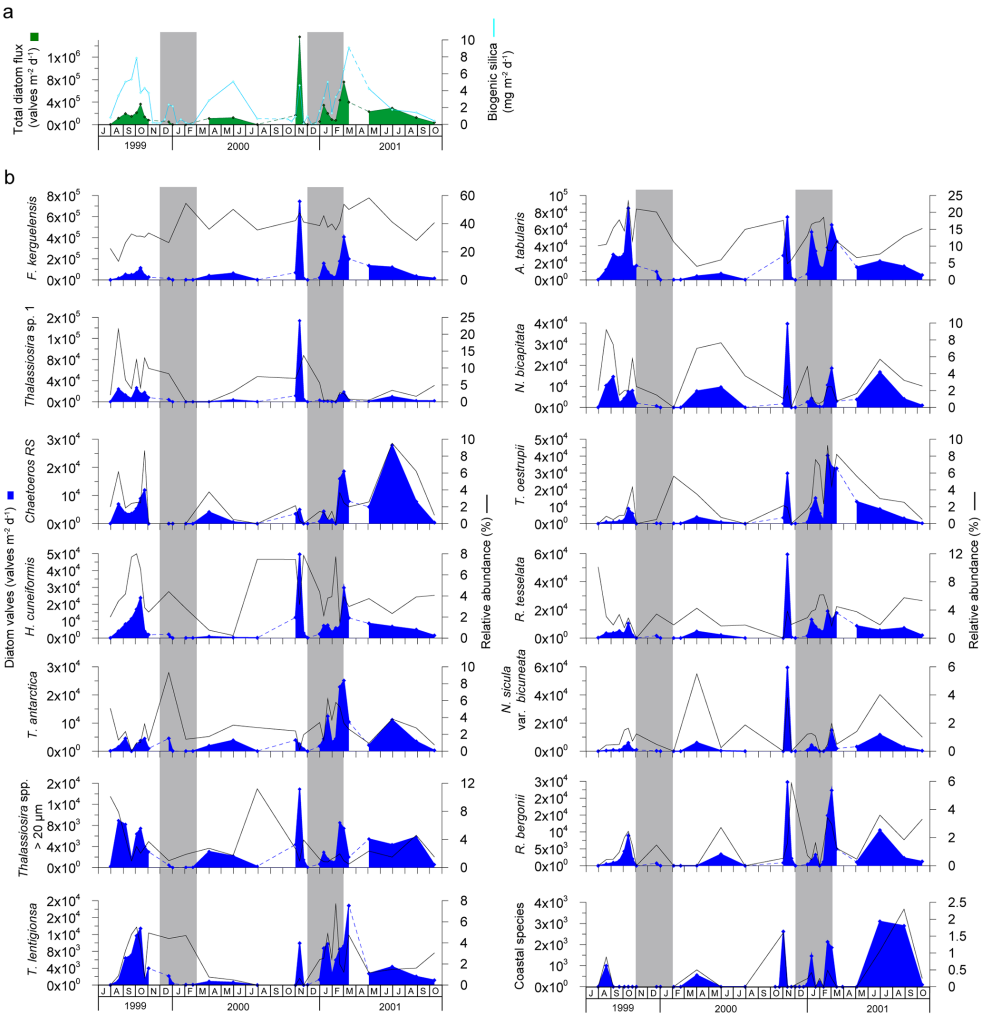

BGD
12, 8615–8690, 2015

Latitudinal and temporal distributions of diatom populations

A. S. Rigual-Hernández et al.

Figure 4. Temporal variability of **(a)** total diatom flux and biogenic silica and of **(b)** flux and relative contribution of the main diatom species at 1000 m at the 47° S site for the period July 1999–October 2001.

BGD
12, 8615–8690, 2015

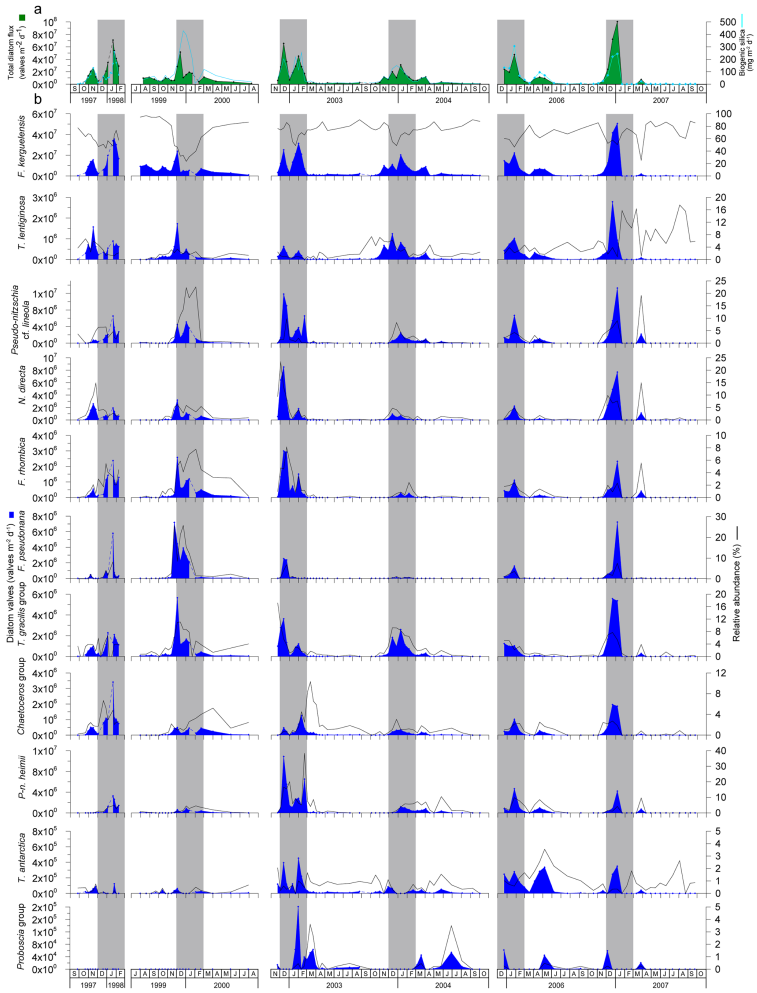

BGD
12, 8615–8690, 2015

Latitudinal and temporal distributions of diatom populations

A. S. Rigual-Hernández et al.

CC BY

Figure 5. Temporal variability of **(a)** total diatom flux and biogenic silica and of **(b)** flux and relative contribution of the main diatom species at 800 m at the 54° S site for the periods July 1999–August 2000, November 2002–October 2004 and December 2005–October 2007.

BGD
12, 8615–8690, 2015

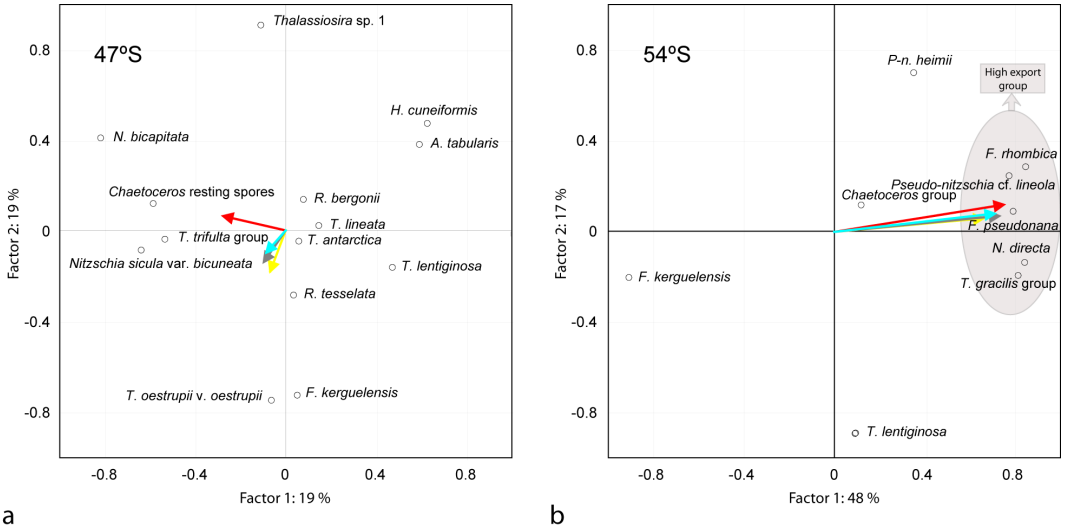

Figure 6. Principal component analysis for the SAZ 47° S **(a)** and PFZ 54° S sites **(b)**. Projection of the variables (diatom species or groups of species accounting for more than 1 % of the integrated assemblage for the whole sampling period) on the first two PCA axes together with total mass (grey), biogenic silica (blue), carbonate (yellow) and POC (red) flux.

BGD
12, 8615–8690, 2015

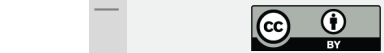

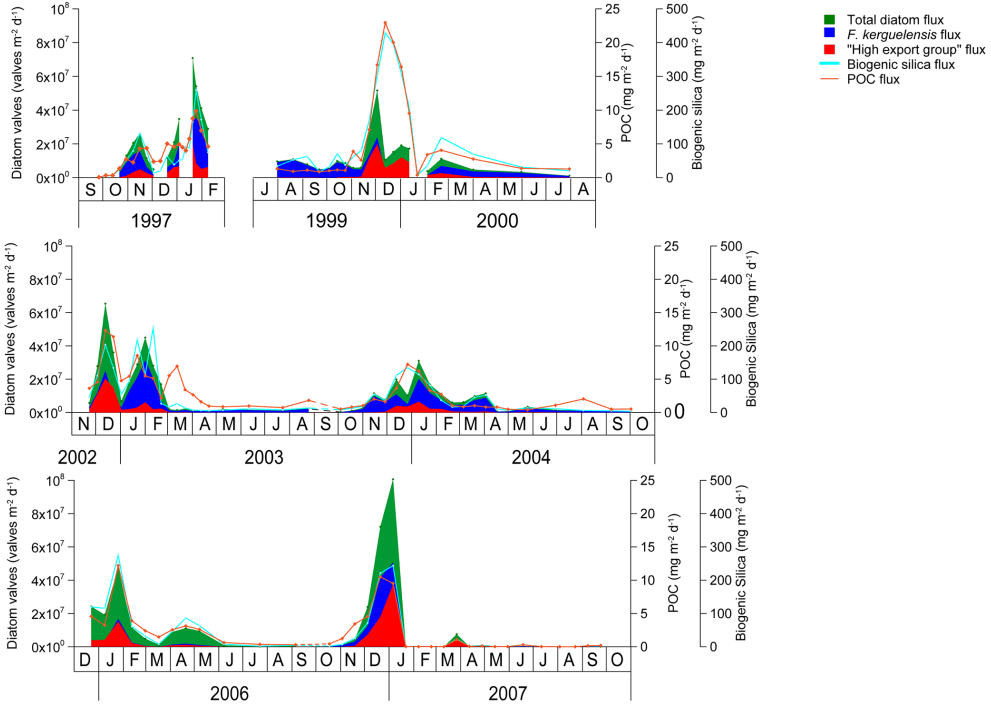

Figure 7. Temporal variability of the total diatom, "High export group", *Fragilariopsis kerguelensis*, biogenic silica and POC fluxes for the six-year record at the 54° S site.

BGD
12, 8615–8690, 2015

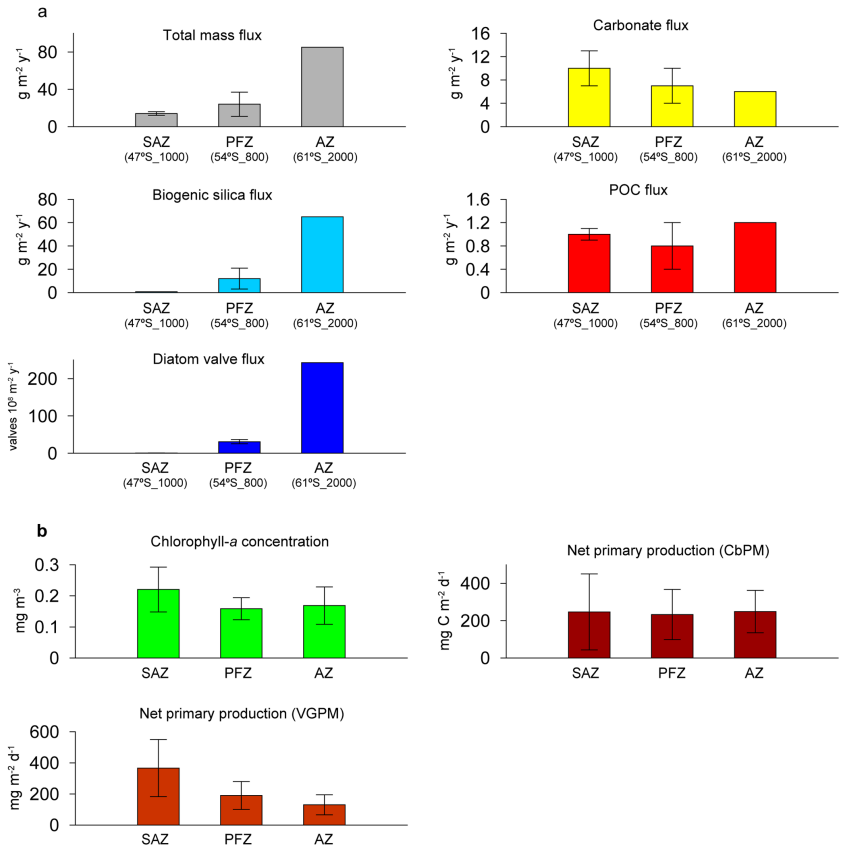

Figure 8. (a) Annual mean total mass, major component, and diatom valve fluxes for the < 1 mm particulate fraction for the 47, 54 and 61° S sites. **(b)** Annual average of Chlorophyll *a* concentration and two different estimates of primary productivity (standard vertically generalized production model – VGPM; and carbon-based production model – CbPM) for the 47, 54 and 61° S sites from October 1997 to September 2007.

BGD
12, 8615–8690, 2015